A COMPARATIVE STUDY ON THE EFFECT OF CLAY LOADING UNDER NORMAL AND AUTO THERMAL EXTRUSION TO THE MORPHOLOGY STRUCTURE AND THERMAL STABILITY OF NYLON 6 NANOCOMPOSITES

FARIDAH BT MOHD NOR

UNIVERSITI MALAYSIA PAHANG

FARIDAH BT MOHD NOR BACHELOR OF CHEMICAL ENGINEERING 2013 UMP

A COMPARATIVE STUDY ON THE EFFECT OF CLAY LOADING UNDER NORMAL AND AUTO THERMAL EXTRUSION TO THE MORPHOLOGY STRUCTURE AND THERMAL STABILITY OF NYLON 6 NANOCOMPOSITES

FARIDAH BT MOHD NOR

A Thesis submitted in fulfilment of
the requirements for the award of the degree of
Bachelor of Chemical Engineering

Faculty of Chemical & Natural Resources Engineering
UNIVERSITI MALAYSIA PAHANG

FEBRUARY 2013

SUPERVISOR'S DECLARATION

"I declare that I have read this dissertation and in
my opinion this thesis is sufficient in terms of scope and
quality for the award of the degree of
Bachelor of Chemical Engineering"

Signature : ……

Name : DR. KAMAL YUSOH

Position : SUPERVISOR

Date : JANUARY 2013

STUDENT'S DECLARATION

I hereby declare that the work in this thesis entitled "*A Comparative Study on the Effect of Clay Loading under Normal and Auto Thermal Extrusion to the Morphology Structure and Thermal Stability of Nylon 6 Nanocomposites*" is the result of my own research except in citied in the references. The project has not been accepted for any degree and is not concurrently submitted for award of other degree.

Signature :…….

Name : FARIDAH BT MOHD NOR

ID Number : KA10152

Date : JANUARY 2013

Special dedication to my supervisor, Dr. Kamal Yusoh for your Time, Guidance, and Support.

And,

To my beloved parents (Mohd Nor bin Hj Ahmad& Khatijah bt Salim) and friends, that encouraged and fully supports me throughout completing this thesis.

ACKNOWLEDGEMENTS

First of all, I would like to express my grateful to ALLAH S.W.T for blessing me with good health, physical and mental. I almost completed my thesis.

I wish to express my thanks and appreciation to Dr. Kamal Yusoh, my supervisor for provided many valuable knowledge, suggestions and constructive critics that greatly influence me and gave me inspire to do this thesis. I also wish to express my sincere gratitude to Mr. Zulhilmi Ismail for gave me plenty of knowledge and comments to improve the quality of my thesis. I also like to express my gratitude for all the lecturers and technical staffs of Faculty Chemical Engineering and Natural Resources, Universiti Malaysia Pahang.

Last but not least, I would like to express my gratitude to all my friends and to staffs in Central Lab and Faculty of Science and Technology (FIST) of Universiti Malaysia Pahang for the assistance with SEM characterization, XRD and TGA analysis

Finally I would like to thank all parties that involved in my thesis, whether directly or indirectly in helping me for their invaluable time, guidance and advice. That support means a lot to me in order to make sure this thesis will be successful. I wish all of you succeed in life and achieve your dream. I hope my thesis will finish with flying colors and I can bring my knowledge to my future career

.

A COMPARATIVE STUDY ON THE EFFECT OF CLAY LOADING UNDER NORMAL AND AUTO THERMAL EXTRUSION TO THE MORPHOLOGY STRUCTURE AND THERMAL STABILITY OF NYLON 6 NANOCOMPOSITES

ABSTRACT

The main purpose of this thesis is to study the influence of auto thermal extrusion on the thermal stability and morphology of fabricated PA6/C20A nanocomposite. The organically modified layered silicates type Cloisite 20A (the montmorillonite modified with a quaternary ammonium salt) and Polyamide 6 (PA6) were used in this research. Fabricated PA6/C20A nanocomposite was prepared by using an auto thermal melt extrusion. The screw speed of twin screw extruder was maintained at constant value of 200 rpm, the clay loadings C20A were varied between 1-5 wt% respectively. The morphological properties were characterized by using both X-Ray Diffraction analysis (XRD) and Scanning Electron Microscopy (SEM), while the thermal stability of obtained PA6/C206 nanocomposite was studied by using thermo gravimetric analysis (TGA). The dispersion and distribution of nanoclays platelets within the polymer matrix, a clay contents show a better role in dictating the quality of extruded PA6/C20A nanocomposite than the auto thermal or conventional setting extruder itself based on the evidently formation number of agglomerated clay. The degradation T_{onset} of PA6/C20A nanocomposite was found to be shifted to the larger value under an auto thermal extrusion. As a conclusion, auto thermal extrusion is suggested as an alternative approach for energy cost reduction and efficiency application in the industry.

KAJIAN PERBANDINGAN KE ATAS KESAN PENAMBAHAN TANAH LIAT SECARA NORMAL DAN AUTO-TERMA TERHADAP STRUKTUR MORFOLOGI DAN KESTABILAN HABA NILON 6 NANOKOMPOSIT

ABSTRAK

Tujuan utama tesis ini ialah untuk belajar mengenai kesan penyemperitan auto-terma terhadap kestabilan haba dan morfologi PA6/C20A nanokomposit. Tanah liat Cloisite 20A (montmorillonite diubah suai dengan suku garam ammonium) dan Polyamide 6 (PA6) telah digunakan dalam penyelidikan ini. PA6/C20A nanokomposit telah disediakan dengan menggunakan satu kaedah auto-terma. Kelajuan skru kembar penyemperitan telah disetkan di nilai konsisten 200rpm, tanah liat C20A yang diletakkan diubah antara 1-5wt% masing-masing. Ciri-ciri struktur dikaji menggunakan analisis Belauan Sinar-X (XRD) dan Imbasan elektron mikroskop (SEM), manakala kestabilan haba PA6/C20A nanokomposit telah dikaji dengan menggunakan analisis termogravimetri (TGA). Rawakan dan pengagihan butiran tanah liat-nano dalam matriks polimer, kandungan tanah liat menunjukkan peranan yang lebih baik dalam menghasilkan kualiti PA6/C20A nanokomposit daripada penyemperitan auto-terma atau penyemperitan biasa berdasarkan pembentukan tanah liat yang terkumpul. Degradasi suhu permulaan PA6/C20A nanokomposit didapati berubah kepada nilai yang lebih tinggi di bawah auto-terma. Konklusi, auto-terma disarankan sebagai satu pendekatan alternatif untuk pengurangan kos tenaga dan kecekapan dalam industri itu.

TABLE OF CONTENTS

LIST OF TABLES

LIST OF FIGURES

LIST OF ABBREVIATIONS

.

C20A	Cloisite 20A
CEC	Cation Exchange Capacity
MMT	Montmorillonite
Nm	Nanometer
OMLS	Organic Modified Layered Silicate
PA6	Polyamide 6
PA66	Polyamide 66
PLS	Polymer layered Silicates
PNC	Polymer nanocomposites
PMMA	Poly (methyl methacrylate)
PS	Polystrene
SEM	Scanning Electron Microscopy
TGA	Thermo Gravimetric analysis
XRD	X-Ray Diffraction

CHAPTER ONE

INTRODUCTION

1.1 Background Research

In recent years, polymer nanocomposites (PNC) have emerged as a new class of material and attracted a number of considerable interest and investment in research and development worldwide. This is largely due to it new and often much improved mechanical, thermal, electrical and optical properties as compared to their macro- and micro-counterparts. These improvements include high modulus, increased strength and heat resistance, decreased gas permeability and flammability, as well as increased biodegradability of biodegradable polymers (Ray and Okamoto, 2003). Traditionally, polymeric materials have always been incorporated with synthetic or natural inorganic compounds in order to improve their properties, or simply to reduce cost.

The polyamide 6/ cloisite 20A nanocomposites exhibited substantial enhancements of the physical properties of the composite relative to the pure polyamide 6 polymer. These physical property improvements include increases in tensile strength, modulus, and heat distortion temperature without loss of impact strength. The enhancement of the impact strength in these composites with substantial increases in strength and stiffness was surprising. Besides that, the water uptake and gas barrier properties of the nanocomposite were substantially improved if compared to pure polyamide (Powell and Beall, 2006).

There are three different types of PLS (Polymer layered Silicates) nanocomposites that are thermodynamically achievable; intercalated nanocomposite, conventional nanocomposite and exfoliated nanocomposite. Polymer–layered silicate nanocomposites, which are the subject of this research, are prepared by incorporating finely dispersed layered silicate materials in a polymer matrix (Fisher, 2003). However, the nanolayers are not easily dispersed in most polymers due to their preferred face to-face stacking in agglomerated tactoids. Dispersion of the tactoids into discrete monolayer is further hindered by the intrinsic incompatibility of hydrophilic layered silicates and hydrophobic engineering plastics. Therefore, layered silicates need to be organically modified initially to produce polymer–compatible clay (organoclay). In fact, it has been well-demonstrated that the replacement of the inorganic exchange cations in the cavities or “galleries” of the native clay silicate structure by alkylammonium surfactants can compatibilize the surface chemistry of the clay and a hydrophobic polymer matrix (Lebaron et al., 1999). Thereafter, different approaches can be applied to

incorporate the ion-exchanged layered silicates in polymer hosts by means of in situ polymerization, solution intercalation or simple direct melt-mixing.

The research is focus on to study a possibility of auto thermal melt compounding as an alternative to a conventional melt compounding in the manufacturing of PNC. A polyamide 6 (PA6) was preferred as base polymer in this research primarily because of the accessibility of this material to the plastic industry. It is naturally already good mechanical, chemical and thermal properties (Okada et al., 1990). The organically modified montmorillonite (MMT) or known as nanoclay namely Cloisite 20A (C20A) is belongs to a group of layered silicate, acts as nano-scaled filler for the composite (Xi et al., 2005). It would be truly interesting to see the thermal stability of fabricated PNC and the exfoliation-rate of platelets including the crystalline behavior of the polymer hybrid after the addition of layer silicate into the pristine polymer under the auto thermal condition as the effectiveness of nanofiller could be influenced by specific melt compounding parameters.

1.2 Problem Statement

A thermal degradation occurred during the compounding processing of PNC. Effect of temperature and an excessive heat originated from high shear stress is determined as an issue that causes degradation in pre-PNC. The influence of an autothermal extrusion on the thermodynamics stability of melt intercalation could have been attracted huge advantages (Vaia et al., 1996).

1.3 Research Objective

Based on the research background and problem statement described in the previous section these are the following objectives in this research:

1.3.1 To compare the thermal stability of fabricated PA6/C20A nanocomposite, that was extruded by using auto thermal and conventional extrusion.

1.3.2 To study the morphological of fabricated PA6/C20A nanocomposite, that was extruded by using auto thermal and conventional extrusion.

1.3.3 To check the possibility of an auto thermal extrusion as an alternative way to reduce the risk of thermal degradation of fabricated nanocomposite.

1.4 Scope Of Research

This research is focusing on the effect of clay loading under conventional and auto thermal extrusion to the thermal stability and the quality of fabricated PNC. The scopes of this research are as below:

1.4.1 To produce fabricated PA6/C20A nanocomposite by combining PA6 and C20A which is the montmorillonite modified with a quaternary ammonium salt.

1.4.2 To produce fabricated PA6/C20A nanocomposite using melt intercalation method.

1.4.3 To characterize the fabricated PA6/C20A nanocomposite samples by using Scanning Electron Microscopy (SEM), X-Ray Diffraction (XRD) and Thermo Gravimetric analysis (TGA).

1.5 Significance Of Research

Fabricated PA6/C20A nanocomposite consisting of PA6 with C20A, have been known to be one of the most valuable applications of nanotechnology. An auto thermal extrusion is predicted to not give any negative influence on the fabricated PA6/C20A nanocomposite. Under auto thermal set-up a material is only allowed to enter the extruder plate once the $\Delta T = 0$. For this purpose, the preheated plates were switched-off throughout the compounding process and only turned on back if the temperature was fallen almost to the minimum tolerance value (224 ± 5 °C). In order to study the influence of an auto thermal extrusion on the thermodynamics stability of PNC, the effectiveness of an auto thermal extrusion by twin-screw extruder should been examined. Besides, to provide a future reference for the organization or person that interested in twin-screw extruder approach in the fabrication of PA6/C20A nanocomposite and to contribute new knowledge in polymer nanotechnology field that is beneficial to environment and automobile industry.

CHAPTER TWO

LITERATURE REVIEW

2.1 Introduction

Polymer nanocomposite is an area of considerable precise interest and of rising industrial practice. Hybrid combinations of natural fillers and polymers were presented to the public for the first time in the 90s (Kojima et al., 1993), a vast market opportunity was forecast: e.g. in 2001 revenues of 4 billion US$ in the US alone were predictable to be achieved in 2010 (Nina, 2002). Benefits of polymer nanocomposites are shown in the improvement of mechanical property (automotive industry, etc.), barrier properties (packaging, film and bottle industry, etc.), contribution to fire retardancy (cable industry, etc.), physical and optical (electronics, batteries).

In general, the thermal processing step of developed nanocomposites requires proper stabilization, which has to be taken into a consideration is the oxidative constancy of the polymer substrate, the influence of the nanofiller as well as the

influence of modifiers and compatibiliser. The nanofillers are most often originated from natural sources such as montmorillonite. In contrast, synthetic mineral clays based from natural origin will, like traditional fillers, have metal ions and other contaminants which influence the thermo oxidative stability negatively.

In order to be fully understood, what really is occurred between the materials in the channel of twin-screw extruder throughout the compounding of polymer, the literatures that specifically talk about the opportunity of mechanical melt compounding of PA6/C20A nanocomposite by an extruder have been reviewed.

2.1.1 Nanotechnology

Nanotechnology is known as one of the most promising areas for technological growth in the 21st century. Nowadays, the impact of nanotechnology could visibly been observed in various sections of knowledge and application which including medicine electronics, fuel cells, solar cells and others (Boisseau and Zhang, 2011). In materials research, the development of polymer nanocomposites is rapidly raising as a multidisciplinary investigate activity whose results could broaden the applications of polymers to the great benefit of many different industries. Polymer nanocomposites (PNC) are polymers (thermoplastics, thermosets or elastomers) that have been reinforced with small quantities (less than 5% by weight) of nano-sized particles having high aspect ratios (L/h > 300) (Denault and Labrecque, 2004).

Nevertheless, a more complete and suitable meaning of nanotechnology is proposed and clearly defined as: The design, characterization, production, and application of structures, devices and system via a controlled manipulation of size and shape at the nanometer range (atomic and molecular scale) that produces structures, devices, and systems with at least one novel or superior characteristic or property (Bawa et al., 2005)

2.1.2 Nanoparticle

Nanoparticles can be three-dimensional spherical and polyhedral nanoparticles (e.g., colloidal silica), two-dimensional nanofibers (e.g., nanotube, whisker) or one dimensional disc-like nanoparticle (e.g., clay platelet). Such nanoparticles offer massive advantages over traditional macro- or micro-particles (e.g., talc, glass, carbon fibers) due to their higher surface area and aspect ratio, improved bond between nanoparticle and polymer, and lower quantity of loading to get equivalent properties.

Nanoparticles are obtained from obtainable natural resources and usually need to be treated because the physical mixture of a polymer and layered silicate may not form a nanocomposite; in this case, a separation into discrete phases takes place. The unfortunate physical interaction between the organic and the inorganic components leads to decrease mechanical and thermal properties. Strong interactions between the polymer and the layered silicate nanocomposites typically lead to the organic and inorganic phases being isolated at the nanometer level. Thus, nanocomposites show unique higher properties than conventional composites (Biswas and Ray, 2001).

2.1.3 Polyamide

Polyamides are widely used materials due to their tunable properties. There are a lot of type polyamides, commercially polyamide being used by industry like polyamide 6 (PA6) and polyamide 66 (PA66). Both of PA6 and PA66 physically differ in terms of glass transition temperature, melting point, crystallinity and tensile modulus among other things. In contrast, PA66 has a melting point of 262°C and glass transition temperature is 65°C which higher than PA6. Meanwhile, PA6 has a melting point of 219°C and its glass temperature is 52°C only. Furthermore, the crystal structure of PA6 is monoclinic while PA66 is triclinic structure and PA66 has tensile modulus is around 2.9 GPa but it is a little lower for PA6 (Chavarria and Paul, 2004). Some of these differences can be traced to the difference in symmetry of their repeats units and to the difference in arrangement of functional units at the chains ends. Obviously, PA6 has a wide range of engineering application for its unique combination of good processibility, higher mechanical properties and chemical resistance. However, its high moisture absorption and low resistance to crack propagation in the presence of a notch have been major limitation for various end use applications. In order to increase these properties, as well thermal stability of PA6, nanocomposite was prepared (Mohanty and Nayak, 2007).

2.1.4 Layered Silicates

Layered silicates used in the synthesis of nanocomposites are natural or synthetic minerals, consisting of very thin layers that are usually bound together with counter-ions. Their necessary building blocks are tetrahedral sheets in which silicon is enclosed

by four oxygen atoms, and octahedral sheets in which a metal like aluminum is surrounded by eight oxygen atoms. Therefore, in 1:1 layered structures (e.g. in kaolinite) a tetrahedral sheet is fused with an octahedral sheet, whereby the oxygen atoms are shared (Chin et al., 2001)

On the other hand, the layered silicate belongs to the group 2:1 phyllosilicates and it is consisted of a small total of magnesium, iron and natrium ion as shown in **Figure 2.1**. Phyllosilicates name is supposed to be originated from Greek word "*phyllon*" which means leaf. Phyllosilicates could be categorized into four different classes (Utrucki, 2004):

i. Serpentine
ii. Clay mineral
iii. Mica
iv. Chlorite

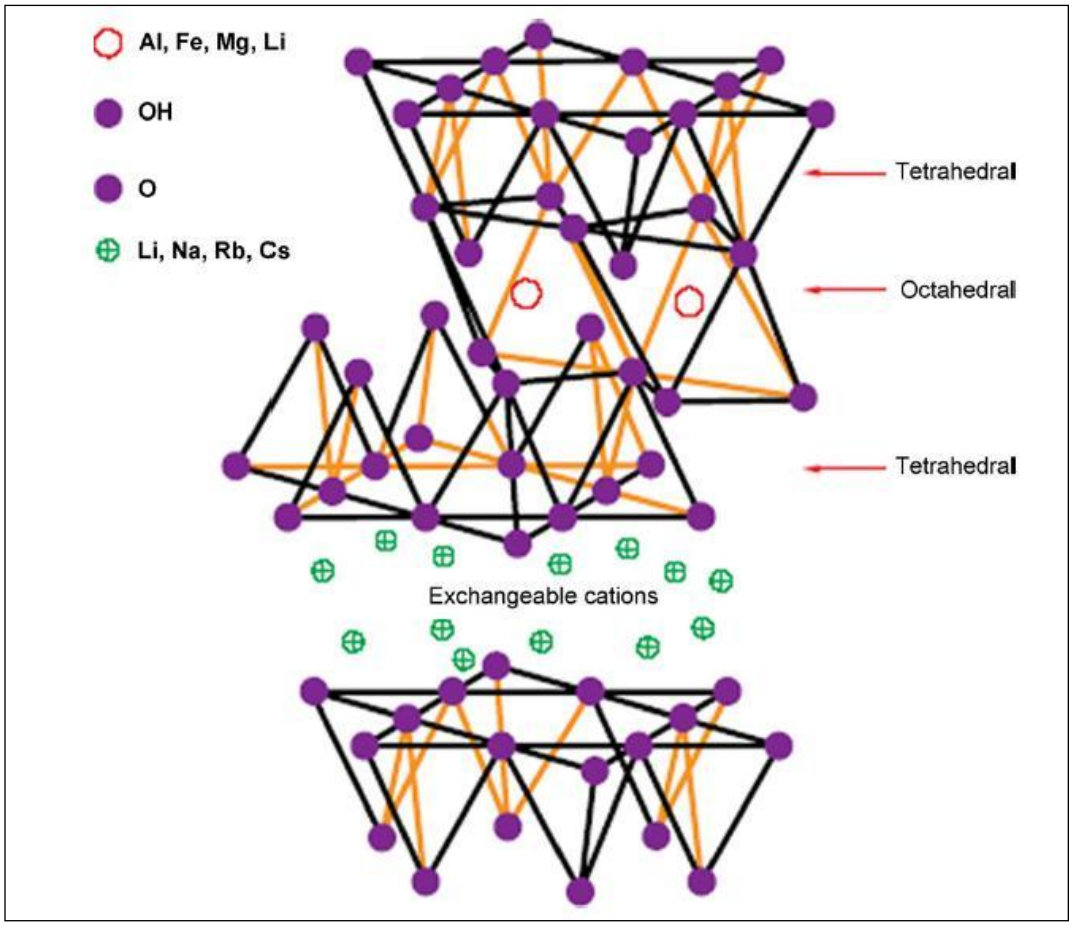

Figure 2.1: The structure of a 2:1 layered silicate

(Source: Beyer, 2002)

Arrangement enabled the ion of oxygen to be interlinked between silica tetrahedral sheets is the arrangement of atoms in the crystal of 2:1 layered silicate composed of two-dimensional layers and a central octahedral sheet of alumina is electrostatic fixed to two external silica tetrahedral by the tip. The thickness of each layer is around 1 nanometer (nm) and lateral dimensions value could have been varied, influenced by the source of the clay and the method of preparation (McNally, 2003) and (Beyer, 2002).

The pyrophillitte could be described as basic 2:1 structure that formed by the silicon in the tetrahedral sheets and aluminum in the octahedral sheet. During substitution of aluminum in the place of silicon in tetrahedral, a structure called mica is obtained, while a montmorillonite structure can be created by replacing the trivalent aluminum cation in the octahedral sheet with divalent magnesium cation. A cation-exchange capacity (CEC) will produce the excess negative charge and the efficiency rate of ion exchange for layered silicate. The CEC for montmorillonite is usually varied between 0.9-1.2 mequiv/g appropriate to the difference origin place of the clay. The sodium and calcium ions exist hydrated in the interlayer to balance the generally negative charge. Consequently, water or polar molecules could break the forces and toward the inside between the units of a layer, follow-on in the expansion of galleries (Chin et al., 2001)

The montmorillonite is classified into a group of clay minerals, known as "smectites" or "smectite clays". In the fabrication of nanocomposite, montmorillonite, hectorite as well as saponite are widely used as clay-filler. The chemical formula is as listed in **Table 2.1**

Table 2.1: Chemical structure of commonly used 2:1 phyllosilicates

Phyllosicates	**General formula**
Montmorillonite	Mx(Al4-xMgx)Si8O20(OH)4
Hectorite	Mx(Mg6-xLix)Si8O20(OH)4
Saponite	MxMg6(Si8-xAlx)O20(OH)4

2.2 Polymer nanocomposite

Polymer nanocomposite materials have attracted great interest because layered clays can highlight almost all types of polymer matrices with similar properties than traditional composites but less weight and better processibility. Varlot et al. (2001) was observed the preparation and characterization of polymer nanocomposites used commercial modified layered silicates. Though, some works dealing with the modification process in order to improve the quality of the nanoclays to produce polymer nanocomposites with improved properties have been published by Kojima et al. (1993). Commonly, modified layered silicates are preserved with several organic onium bases, and in peak of the modification processes around 2–5% weight of solids is used, in order to reduce the viscosity and get a more homogenous solid solution. Isomorphic substitution within the layers generates a negative charge, defined through the cation-exchange capacities (CEC). This excess of negative charge is balanced by cations (Na^{+}, Ca^{2+}, and Li^{+}) that exist hydrated in the interlayer (Kojima et al., 1993). To render nanoclays miscible with polymers one must exchange the alkali counterions with cationic surfactants, such as alkylamonium. While an excess of surfactant is normally used to complete the interchange reaction, the properties of the final polymer nanocomposite can reduce.

Furthermore, a polymer composite is combination of layered clays and a polymer matrix, which either conventional composite or nanocomposite see **Figure 2.2** can be formed depending on the nature of the components and processing conditions. Conventional composite is obtained if the polymer cannot intercalate into the galleries of

clay minerals. The properties of such composite are similar that of polymer composites reinforced by micro particles. There are two extreme nanostructures resulting from the mixing of clay minerals and a polymer provided that is a favor conditions. One is intercalated nanocomposite (I), in which monolayer of extended polymer chains inserted into the gallery of clay minerals consequential in a well prepared multilayer morphology stacking alternately polymer layers and clay platelets and a repeating distance of a few nanometers. The other is exfoliated or delaminated nanocomposite (II), in which the clay platelets are completely and uniformly dispersed in a continuous polymer matrix .On the other hand, it should be noted that in most cases the cluster (so-called partially exfoliated) nanocomposite (III) is common in polymer nanocomposites.

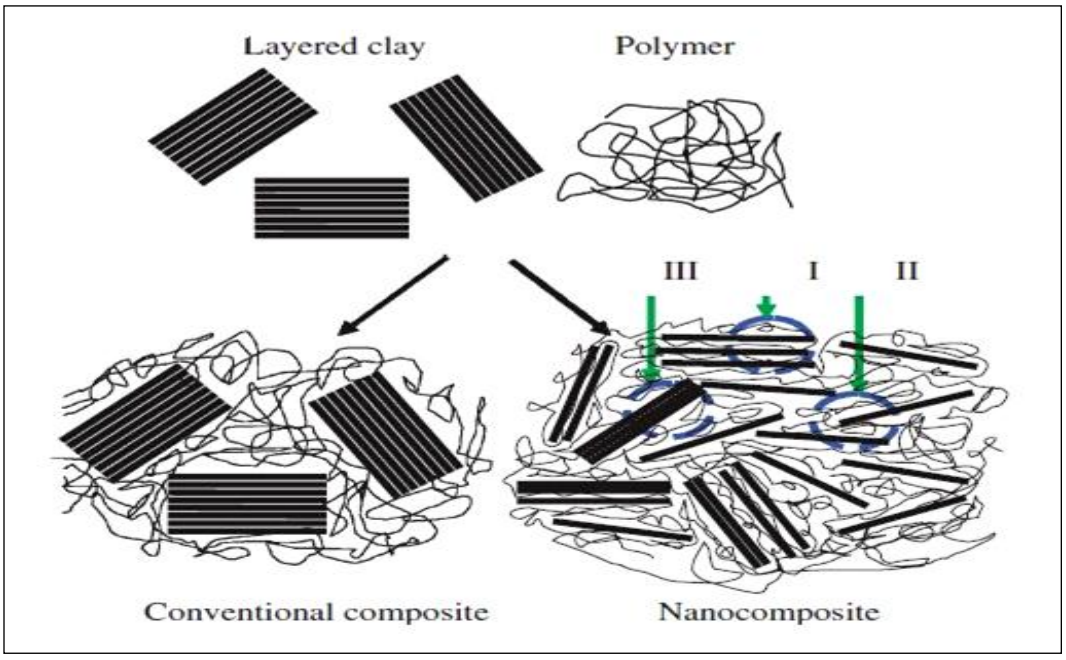

Figure 2.2: Illustration of clay-based polymer composites, including conventional Composite and nanocomposite with intercalated (I), exfoliated (II) or cluster (III) structure

(Source: Zeng et al., 2005)

2.3 Polymer layered silicate nanocomposite

In general, polymer/layered silicate (PLS) nanocomposites have three different types: intercalated nanocomposite, exfoliated nanocomposite and conventional nanocomposite, which are thermodynamically achievable as shown in **Figure 2.3**.

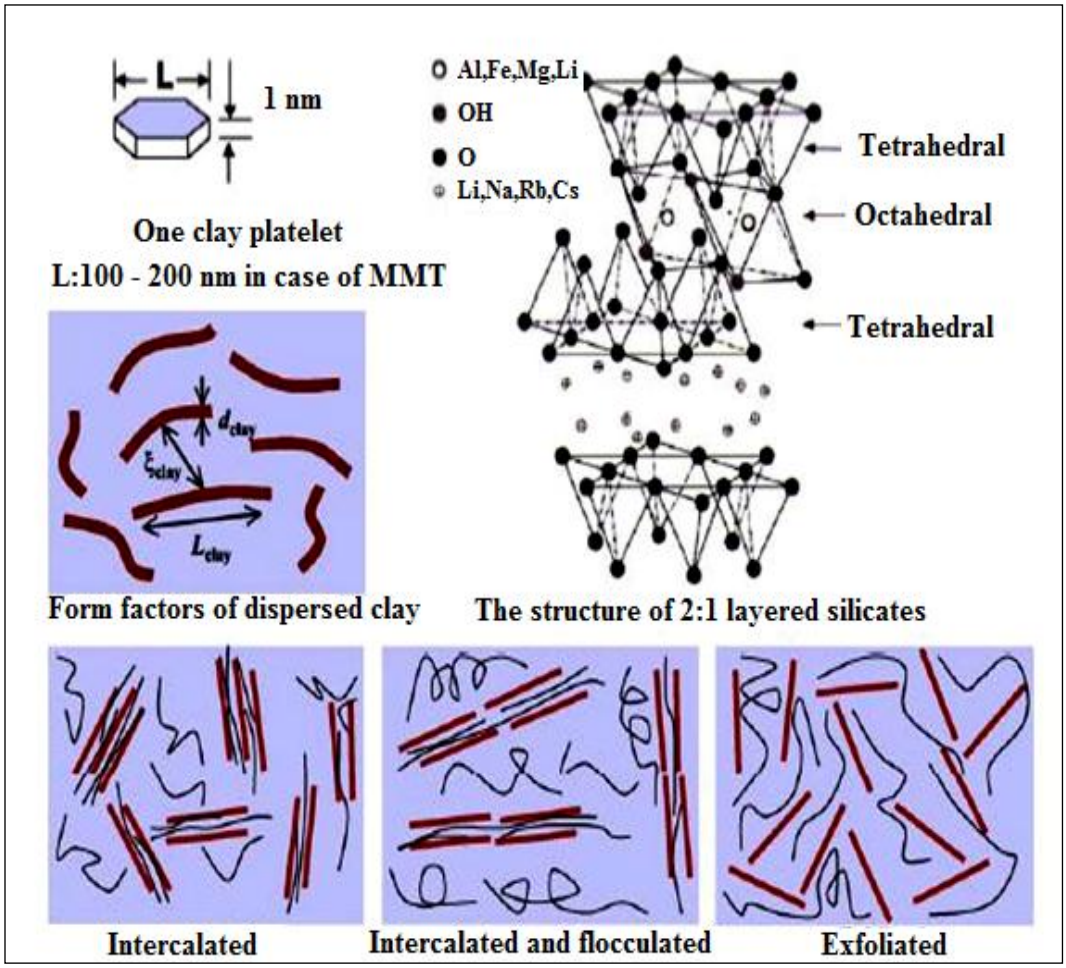

Figure 2.3: Schematically illustration of three different types of thermodynamically achievable PLS nanocomposite

(Source: Ray et al., 2003)

There are two particular characteristic of layered silicates that are commonly considered for PLS nanocomposites. The first is the ability of the silicate particles to disperse into individual layers. The second characteristic is the ability to fine tune their surface chemistry through ion exchange reactions with organic and inorganic cations. These two characteristics are interrelated since the degree of dispersion of layered silicate in a particular polymer matrix depends on the interlayer cation

2.3.1 Intercalated nanocomposite structure

The addition of a polymer matrix into the layered silicate structure occurs in a crystallographically normal fashion, not considering of the clay to polymer ratio in intercalated nanocomposites. Intercalated nanocomposites are generally interlayer by a few molecular layers of polymer. Properties of the composites typically look like those of ceramic materials. Furthermore, intercalation causes less than 20-30 A separation between the platelets (Alexandre, 2000). The majority of the polymer nanocomposite was found to have intercalated nanocomposite structure because the silicate layers are highly anisotropic with lateral dimensions ranging from 100 to 1000 nm. Moreover, when separated by large distances (i.e. when delaminated) cannot be placed completely randomly in the structure of polymer (Chin et al., 2001). In intercalated nanocomposite also, the unit cells of clay structure are expended by the insertion of polymer into the interlayer spacing while the periodicity of the clay structure is maintained.

2.3.1 Exfoliated nanocomposite structure

In an exfoliated nanocomposite, by an average distances that depends on clay loading the individual clay layers are separated in a continuous polymer matrix. Frequently, the clay content of an exfoliated nanocomposite is much lower than that of an intercalated nanocomposite. There is a general agreement in the literature that exfoliated structures lead to better mechanical properties, mostly higher modulus, than intercalated nanocomposites (Jordan et al., 2005). In **Figure 2.4,** Fischer (2003) reported that polymers surface active agents favor in a subsequent separation of the platelets from each other forming finally the matrix material with homogeneously dispersed platelets (molecular composites).

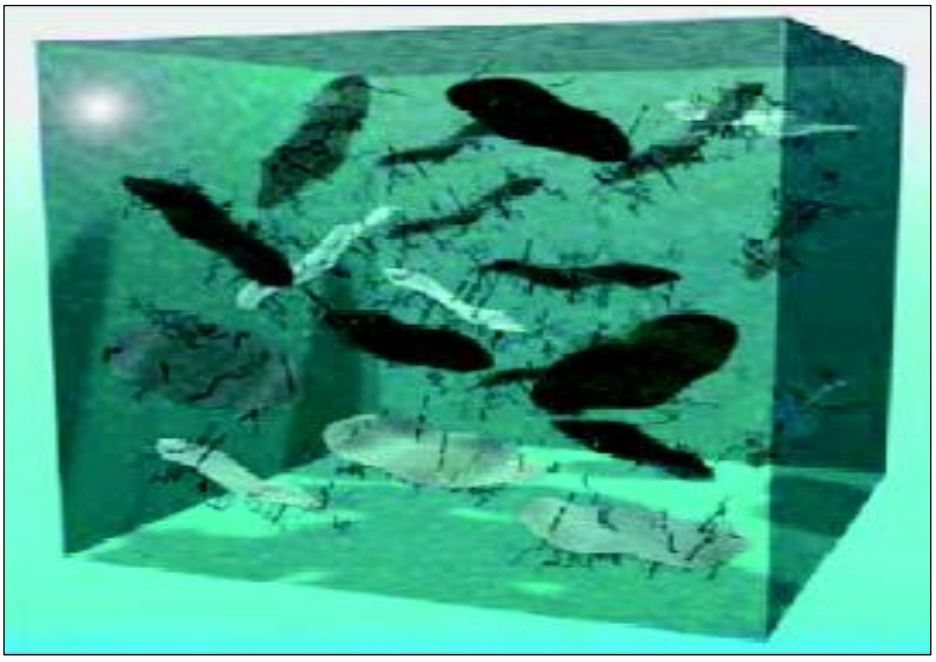

Figure 2.4: polymer-clay nanocomposite material with completely exfoliated (molecular dispersed) clay sheets within the polymer matrix material

(Source: Fischer, 2003).

Moreover, the exfoliation of layered minerals and the preparation of a homogeneous nanocomposite material are totally hindered by the fact that sheet like material display a strong tendency to agglomerate due to their big contact surfaces (Denault and Labrecque, 2004). Nevertheless, the crystal structure of the clay for exfoliated nanocomposite is completely exfoliated by individual dispersion of the clay layers into the polymer matrix (Yusoh et al., 2010). There is a number of methods to increase a degree of exfoliation in a nanocomposite, such as in situ polymerization, melt blending, solution blending, sonication, high shear mixing and melt intercalation (Kudyakov et al., 2009).

2.3.3 Conventional nanocomposite structure

Theoretically this is same as intercalated nanocomposites. Nevertheless, silicate layers are sometimes flocculated suitable to hydroxylated edge–edge contact of the silicate layers. Likewise, a conventional nanocomposite is widely used and already recognized its role in the broad spectrum of consumerism whether by industry or housewives. Then, the higher loading of nanofiller required by conventional nanocomposite in order to achieve the same characteristic as a nanocomposite obviously shows the weakness of unadventurous feature of normal composite. This higher contain of nanofiller more frequently than not lead to increase of viscosity, weight, brittleness and opacity which could conquest the purpose of manufactured composite itself (Alexandre, 2000). As a result, conventional nanocomposite has poor physical interaction between the organic and the inorganic components lead to poor mechanical and thermal properties (Biswas and Ray, 2001)

2.4 Preparation of polymer nanocomposite

2.4.1 Introduction

There are several processes to make clay-based polymer nanocomposite including in-situ intercalative polymerization, solution intercalation and melt intercalation. As shown in **Figure 2.5** each technique consists of several steps to achieve polymer nanocomposites and begins with organoclays or sometimes pristine clays.

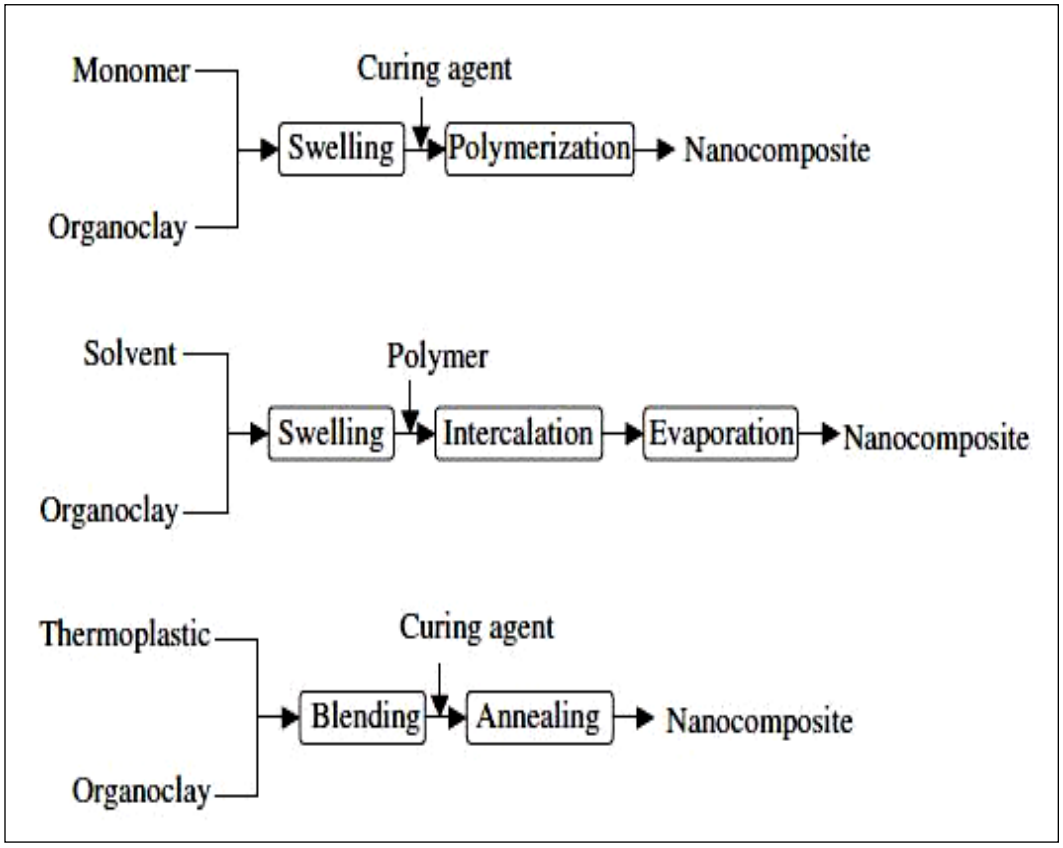

Figure 2.5: Flowchart of three processing techniques for clay-based polymer nanocomposites: in-situ polymerization (upper), solution intercalation (middle) and melt intercalation (bottom)

(Source: Yano et al., 1997)

The formation of polymer nanocomposites is driven by different forces depending on the technique used, and each technique has its advantages and disadvantages as summarized in **Table 2.2**.

Table 2.2: Processing techniques for clay-based polymer nanocomposites

(Source: Zeng et al., 2005)

Processing	Drive force	Advantages	Disadvantages	Examples
In-situ polymerization	Interaction strength between monomer and clay surface; Enthalpic evolvement during the interlayer polymerization	Suitable for low or non-soluble polymer;A conventional process for thermoset nanocomposite	Clay exfoliation depends on the extent of clay swelling and diffusion rate of monomers in the gallery; Oligomer may be formed upon incompletely polymerization	Nylon 6, epoxy, polyurethane, polystyrene, polyethylene oxide, unsaturated polyesters, polyethylene terepthalatate
Solution exfoliation	Entropy gained by desoption of solvent, which compensates for the decrease in conformational entropy of intercalated polymers	Prefer to water soluble polymer	Compatible polymer clay solvent system is not always available ; Use of large quantities of solvent; Co-intercalation may occur for solvent and polymer	Epoxy, polyimide, polyethylene, poly-methylmethacry-late

Table 2.2 **(continue)**

Melt intercalation	Enthalpic contribution of the polymer organoclay interactions.	Environmental benign approach; No solvent is required; Nanocomposite can be processed with conventional plastic extrusion and molding technology	Slow penetration (transport) of polymer within the confined gallery	Nylon 6, Polystyrene, polyethylene terephthalate

2.4.2 In-situ intercalative polymerization

The unprecedented mechanical properties of nylon6/clay nanocomposite synthesized by this technique were first established by researchers at the Toyota Central Research Laboratories (Kojima et al., 1993).The polymer is produce in the presence of the clay and in most cases is tethered to the clay surfaced. Initiation of polymerization by heating or radiation or by diffusion of suitable initiator between the layered silicates is swollen within the monomer or monomer solutions as shown in **Figure 2.6**. So the polymer formation can occur between the intercalated sheets. The in-situ polymerization technique have been reported in many literatures such as cationic polymerization (Xu et al., 2006), ring opening polymerization (Kubies et al., 2002) and conventional free radical polymerization (Simoes et al., 2009). The resulting layered silicate synthesized from this method is normally possessed unorganized structure which takes place after

the intra and extra-interlayer polymerization reached an equilibrium state (Alexandre, 2000) and (Beyer, 2002)

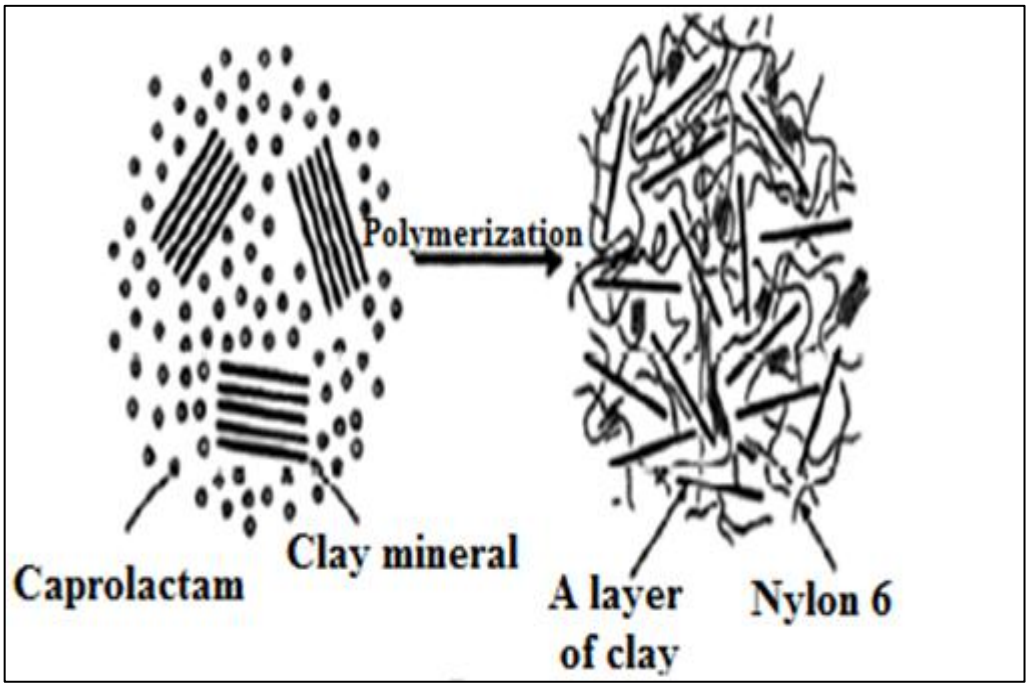

Figure 2.6: Synthesis of Nylon-6/clay nanocomposites

(Source: Ray and Okamoto, 2003).

2.4.3 Solution intercalation method

This method required for both of the inorganic nanofiller and the organic polymer to be in solution form. Followed by its mixture with polymer or prepolymer after the layered host is to be swelled in a solvent (water, toluene, etc.), where by the chains of the latter intercalate while displacing the solvents used for swelling. Polymer layered nanocomposite outcome when the solvent within the interlayer is removed, as

shown in **Figure 2.7.** Due to this reason, not many polymers are suitable to be used in this method since only water-soluble polymer such poly vinyl alcohol (Greenland, 1963) and organoclay dispersed in chloroform (Wang et al., 1998). The disadvantage of this method in order to be considered as a main fabrication strategy for the commercialization of PNC is because of the large quantity of toxic, poisonous solution needed for the synthesizing of polymer nano-hybrid itself and environmental unfriendly (Alexandre and Dubois, 2000).

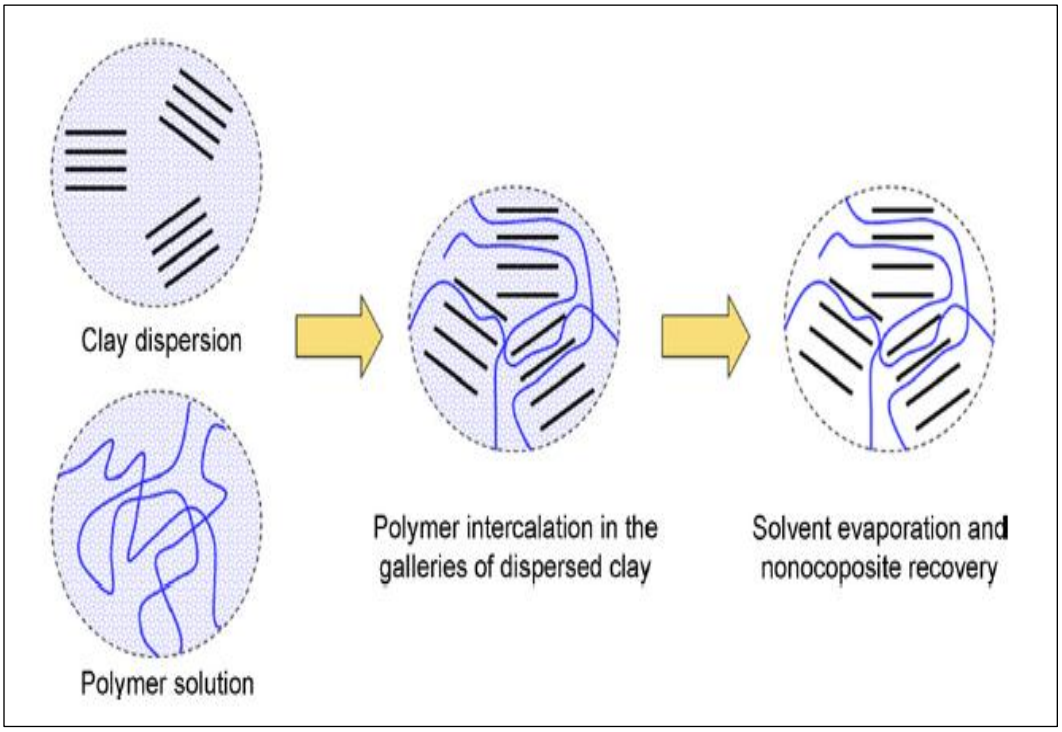

Figure 2.7: PLS obtained by intercalation from solution

Aranda and Ruiz (1992) applied this method for preparation of polyethylene oxide (PEO) /MMT nanocomposites. In solution intercalation method the nature of solvents is critical in facilitating the insertion of polymers between the silicate layers,

polarity of the medium being a determining factor for intercalations (Rausell and Serratosa, 1987).The high polarity of water causes swelling of Na^{+}-MMT, provoking cracking of the films. Methanol is not suitable as a solvent for high molecular weight (HMW) PEO, whereas water/methanol mixtures appear to be useful for intercalations, although cracking of the resulting materials is frequently observed. However, they realized that PEO/silicate materials show good stability toward treatment with different solvents such as acetonitrile, methanol, ethanol and others.

2.4.4 Melt Intercalation

Melt intercalation is an environmentally compassionate one, uses all types of polymers as well as being compatible. It is due to it has tremendous potential for industrial processes such as injection molding, being the most popular procedure to prepare nanocomposites for industrial applications. Hence, there are many advantages to direct melt intercalation than solution intercalation. In this method, polymers, and layered hosts are annealed above the softening point of the polymer see **Figure 2.8**.The driving force for this mechanism is important enthalpy contribution of the polymer/organoclay interaction during blending and annealing steps (Zaikov et al., 2005).

Based on study by Giannelis et al. (1993), polystrene (PS) was the first polymer used for the preparation of nanocomposite using this method with alkylammonium cation modified MMT. In typical preparative method, PS was first mixed with the host

organic modified layered silicate (OMLS) powder and the mixture was pressed into pellet. Next, heated under vacuum at 165°C which temperature is well above the bulk glass transition temperature of PS. Ensuring the presence of a polymer melt. In spite of that, a different research work through this method for the preparation of ethylene-vinyl alcohol copolymer/OMLS nanocomposite was claimed as successful (Artzi et al., 2002) and suitable for the preparation of liquid crystal polymer (DHMS7,9) based nanocomposite (Vaia and Giannelis, 2001).

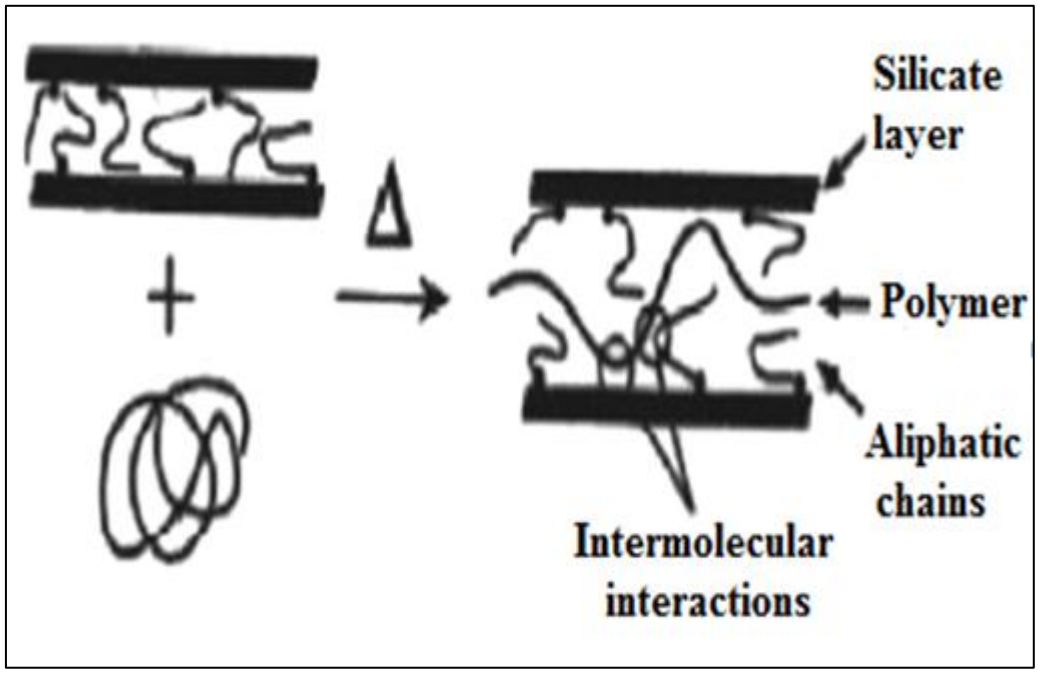

Figure 2.8: Schematic depicting the intercalation process between a polymer melt and an organic modified layered silicate

(Source: Ray and Okamoto, 2003).

2.5 Extruder

The first extruder machine ever recorded in any literature in any literature was pioneered in 1847 by H.Bewley in England, which manufactured under the company of Gutta-Percha Company as shown in **Figure 2.9**. The extruder could be classifying into two types which are single screw and twin-screw extruder. Single screw extruder is generally used in many plastic sectors due to the low cost in acquiring and maintaining a single screw extruder. In addition, the simplicity of the components and construction parts of a single screw extruder also does not necessitate a need for an expert to be consulted (Kolter, 2010).

Besides, in term of plastic manufacturing efficiency and flexibility, twin-screw extruder presented more to the plastic manufacturer by providing an easier material feeding system, higher dispersive mixing and kneading potential, less risk of overheating of extruded material as well as shorter and consistent residence time distribution in extruder as compared to a single screw extruder (Crowley, 2007).

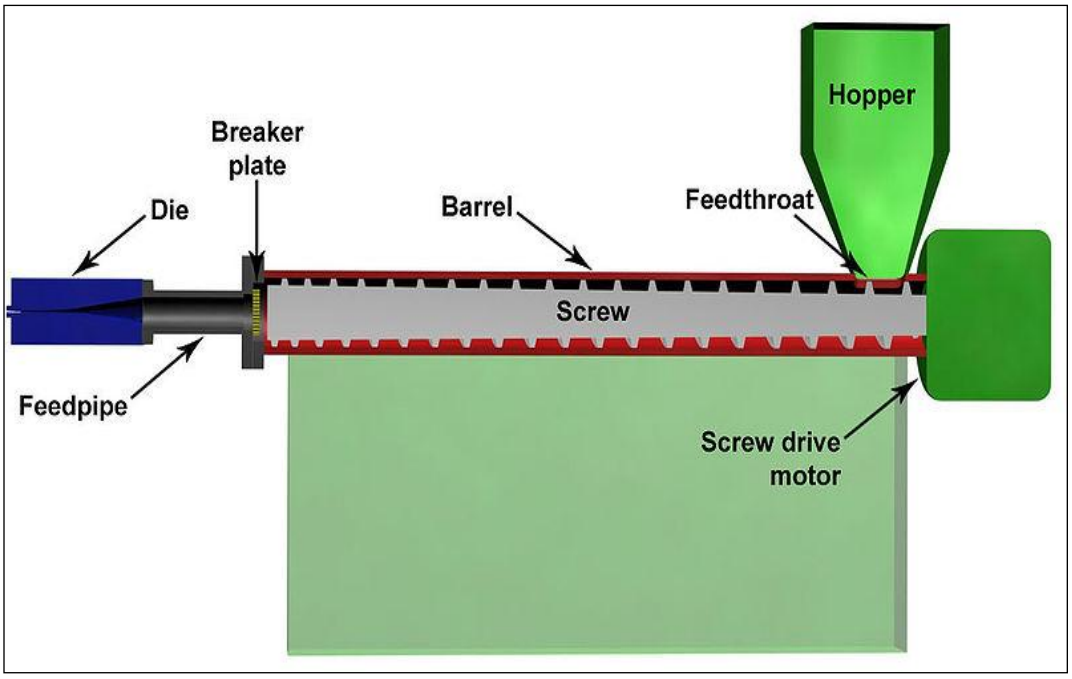

Figure 2.9: Extruder Section

2.5.1 Melt Intercalation by an extruder

Other than that, under melt intercalation by extruder the polymer is heated at pre-determined temperature. Followed by an intercalation/exfoliation phase throughout determination of layered silicates that usually is took stage during molten state of polymer after set up above the melting point of the polymer. In this method, dispersion ability either by a dispersive mixing or distributive mixing is established from the shear rate produced, where the shear force itself could be determined from the screw design and extruder type. The exfoliation rate could be additional increased by utilizing mixer, extruder or sonicator (Vaia et al, .1996). Fornes et al. (2001) prepared PA6/OMLS nanocomposite in the molten state using a twin-screw extruder. They used three different

molecular grades of PA6 for the preparation of nanocomposite with bis (hydroxyethyl) (methyl)-rape seed quaternary ammonium [(HE) 2M1R1] modified MMT, and attempted to determine the effects of matrix molecular weights on structure, properties, and rheology.

2.5.2 Auto thermal Extrusion

Other strategy of extrusion is an auto thermal extrusion where the extrusion is allows running after the pre-heat on the considered set of barrel temperature is completed. This run of extrusion is relied absolutely on the driving energy of extruder without the support of heat from any heating element. In other to compounding of PNC by auto thermal extrusion, the heat experienced by the molten polymer in extruder could be on top is generated through the rotation of extruder screw and uniformly be dispersed throughout the extruded material. Consequently from this process, the risk of thermal decomposition and degradation of organic polymer and inorganic filler imposingly could be greatly reduced while at the same time, an even temperature supply characteristic in an extruder is effectively accomplished (James, 1954).

To operate an extruder auto thermal, it must be possible to deform and shear the solid plastic at low temperatures and thereby generate sufficient internal heat to cause it to melt. Polyethylene is an example of a plastic that can be extruded auto thermal Bernhardt and McKelvey (1954), have recently reported the results of an intensive investigation of the application of the auto thermal principles to polyethylene

plasticating extrusion. The resulting development of high speed and high capacity auto thermal extrusion processes for polyethylene are perfectly feasible, and that the melt theory will prove very useful in this development. Furthermore, it appears that the development of truly auto thermal plasticating extrusion processes for some of the other plastics will not be achievable. PA6, for example, is hard and rigid at room temperature and therefore is very difficult to work in a screw extruder. In PA6 extrusion the melting is really caused by transferred heat and PA6 extrusion is mainly a heat transfer controlled process. This may be an inherent limitation to the development of high capacity extrusion processes for it and similar materials.

2.5.3 Conventional Extrusion

Conventional extrusion means that heating elements of extruder was allowed to be continuously switched-on during the compounding of PNC. The temperature profile of a twin screw extruder with constant, ascending and descending is supposed to have a say on the quality of produced nanocomposite. Throughout handle this extruder, care must be exercised in ensuring that only dry material is used. Failure to ensure adequate drying can lead to product deformities, surface finish, dimensional control and porosity. This run of extrusion is widely used and already established its role in the broad spectrum of consumerism whether by industries or even by a housewives. The higher loading of nnofiller required by this extrusion in order to achieve the same characteristic as a nanocomposite clearly shows the weakness of conservative feature of ordinary composite (Alexandre, 2000)..

2.6 Characterization

Commonly, the structure and dispersion of PA6/C20A nanocomposites has typically been established by using X-Ray Diffraction (XRD) analysis combines with Scanning Electron Microscopy (SEM) analysis. The most challenging parts in characterizing nanocomposites are quantifying the levels of dispersion and exfoliation. On the other hand, the combination of SEM analysis and XRD appears to be more global method to quantify levels of dispersion and exfoliation when coupled with SEM analysis for image confirmation (Salahuddin, 2001).

2.7 Thermal Analisis

The thermal stability of polymer composites is usually estimated from the weight loss upon heating which consequences in the formation of volatile products. In polymer nanocomposites, the presence of clay platelets which delay the diffusion of volatiles and support the formation of char after thermal decomposition improved thermal stability. Thermal analysis techniques are widely used for polymer because these methods are sensitive to structural change, which are suitable for substances that composed of large and extended molecules (Sepe, 1997). The most common n for thermal analysis on the polymer nanocomposite is Thermo gravimetric analysis (TGA)

2.7.1 Thermogravimetric Analysis (TGA)

TGA is an analytical method that determines changes in weight in relation to change in temperature. TGA is usually in use in research and testing to find out characteristics of materials such as polymers, to determine degradation temperatures, absorbed moisture content of materials and others (Sepe, 1997). A sample is loaded against a pan and place on the balance. A furnace then encloses the sample and the temperature can be increase at a given rate and in a given environment. The constituents of the sample will be burn off at unusual rates making the weight percent of the constituents determinable. On the other hand, Blumstein (1965) first presented the improved thermal stability of a PLS nanocomposite that combine poly (methyl methacrylate) (PMMA) and montmorillonite (MMT) clay. These PMMA nanocomposite were prepared by free radical polymerization of MMA intercalated in the clay. He revealed that the PMMA that was intercalated (*d* spacing increase of 0.76 nm) between the galleries of MMT clay resisted the thermal degradation under conditions that would then fully degrade pure PMMA. TGA data shown that both linear and cross linked PMMA intercalated into MMT layers have a 40-50°C greater decomposition temperature. Blumstein claims that the stability of the PMMA nanocomposite is due not only to its different structure, but also to the limited thermal motion of the PMMA in the gallery.

Based on the experimental TGA results (Fornes et al., 2003), the rate of degradation of PA6 during the melt processing of PA6/C20A nanocomposite could be

correlated to the decomposition of surfactant itself. The structure of alkyl ammonium modifier is considered as a factor in the degradation of surfactant. The HE groups on nitrogen shows more stable organoclay and less degradation of PA6 compared to methyl group (M3T1 against (HE) 2M1T1). However, this thermo gravimetric analysis test is run under no influenced of shear stress/strain, which is considered as one of factors that contributed to the degradation of surfactant (Vanderhart et al., 2001)

2.8 Morphology Analysis

2.8.1 X-ray Diffraction (XRD) Analysis

The atomic planes of a crystal cause an incident beam of X-rays to interfere with one another as they leave the crystal. The phenomenon is called X-ray diffraction, shown in **Figure 2.10**. Therefore using XRD in particular wide angle, XRD is the most commonly used technique for examining the structure and occasionally for studying the process kinetics of polymer nanocomposites. The position, shape, and intensity of the basal reflections of XRD patterns of the materials are monitored, in order to study intercalated or exfoliated nanostructure .For example, the extensive layer separation in an exfoliated nanocomposite is reflected in the disappearance of any coherent XRD whereas the finite layer expansion in an intercalated nanocomposite is related with the appearance of a new basal reflection corresponding to the larger gallery height. Unfortunately, such technique cannot provide the spatial distribution of the clay layers

or structural non-homogeneities in nanocomposites. The information from XRD patterns is unfortunately not enough to make known the formation mechanism and ultimate structure of nanocomposites (Krishnamachari et al., 2009)

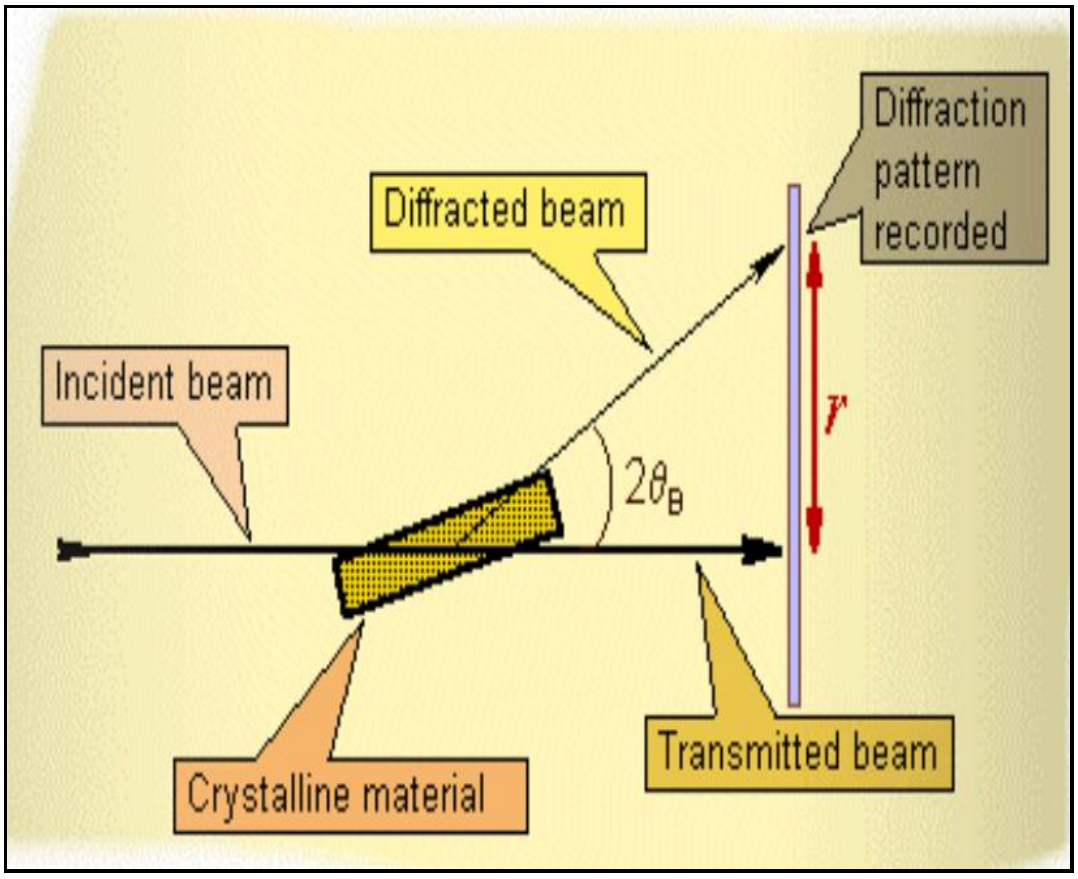

Figure 2.10: Phenomenon XRD

(Source: www.micro.magnet.fsu.edu/primer/java /interference/index.html)

Besides that, XRD compromises a suitable method to determine the interlayer spacing of the silicate layers in the original layered silicates and in the intercalated nanocomposites (within 1–4 nm), slight the spatial distribution of the silicate layers and any structural non-homogeneities in nanocomposites. Also, some layered silicates

initially do not show well-defined basal reflections. Thus, peak increase and intensity decreases are very challenging to study scientifically (Ray et al., 2002). Consequently, conclusions concerning the mechanism of nanocomposites formation and their structure based exclusively on XRD arrangements are only uncertain. Nevertheless, extraordinary care must be exercised to guarantee an illustrative cross-section of the sample. In such intercalated nanocomposites, the repetitive multilayer structure is well preserved, allowing the interlayer spacing as shown in **Figure 2.11**. In contrast, the extensive layer separation associated with exfoliated structures disrupts the coherent layer stacking and results in a featureless diffraction pattern. Thus, for exfoliated structures no more diffraction peaks are visible in the XRD diffractograms either because of a much too large spacing between the layers (greater than 8 nm in the case of ordered exfoliated structure) or because the nanocomposite does not present ordering (Utrucki, 2004).

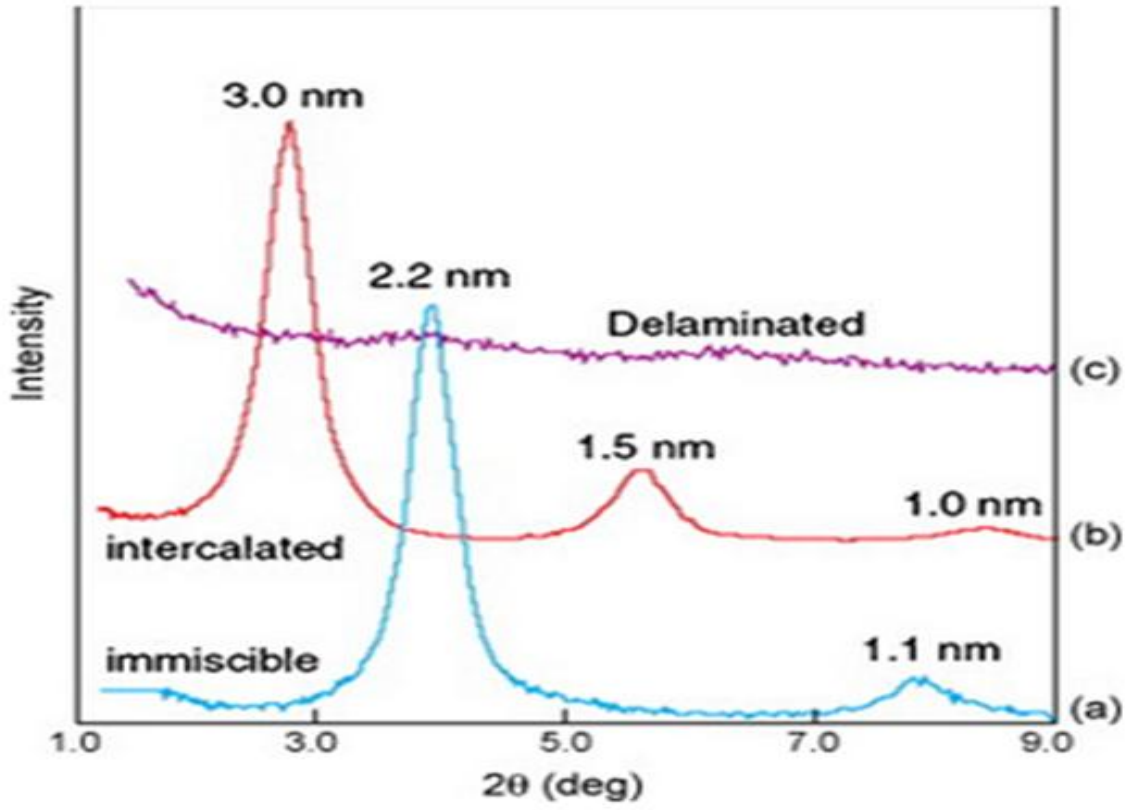

Figure 2.11: Typical XRD patterns from polymer/layered silicates: (a)PE + organoclay (b) PS + organoclay (c) siloxane + organoclay

2.8.2 Scanning Electron Microscopy (SEM)

Generally, the structure of nanocomposite has typically been well-known using SEM observation. SEM could allow surface roughness and morphology dispersion degree of clay particles. On the other hand, spatial delivery of the various phases and views of the defect structure through direct visualization. However, special care must be exercised to guarantee a representative cross-section of the sample. SEM is essential technique for evaluating nanocomposite structure (Morgan and Gilman, 2003).

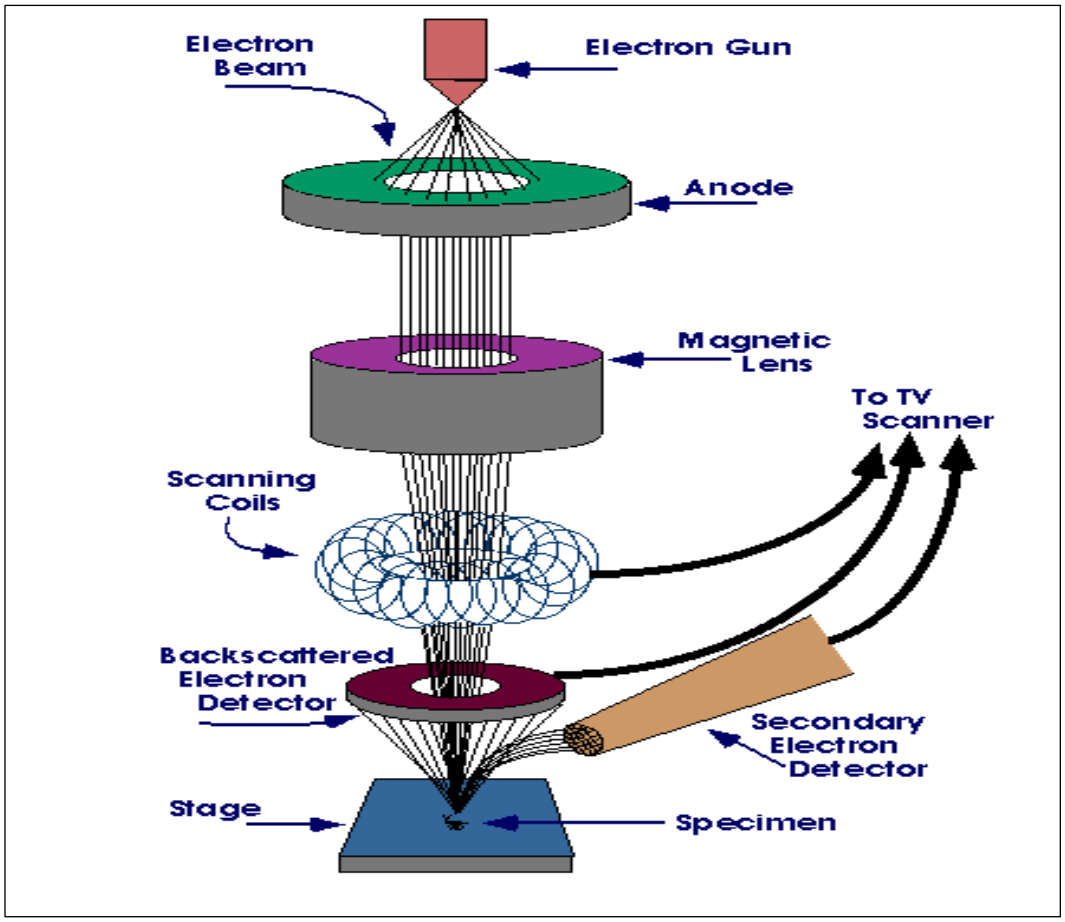

Figure 2.12: Diagram of SEM

Likewise, SEM is an instrument that produces a largely magnified image by using electrons instead of light to form an image. A beam of electrons is formed at the top of the microscope by an electron gun. At that time, the electron beam follows a vertical path through the microscope, which is held within a vacuum. The beam travels through electromagnetic fields and lenses, which focus the beam down toward the sample. Once the beam hits the sample, electrons and X-rays are emitted from the sample (Clarke, 2002).

CHAPTER THREE

RESEARCH METHODOLOGY

3.1 Introduction

In order to prove the problem statement, there are few methods that have to be followed. First of all, the synthesizing of PA6/C20A nanocomposite by melt intercalation method. Melt intercalation is an environmentally compassionate one, uses all types of polymers as well as being compatible. It is due to it has tremendous potential for industrial processes such as injection molding, being the most popular procedure to prepare nanocomposites for industrial applications. Next, the samples are characterized based on morphological analysis by using XRD and SEM. Therefore using XRD in particular wide angle, XRD is the most commonly used technique for examining the structure and occasionally for studying the process kinetics of polymer nanocomposites. Generally, the structure of nanocomposite has typically been well-known using SEM observation. SEM could allow surface roughness and morphology dispersion degree of

clay particles. Then, it is followed then by using TGA to make thermal analysis. TGA is an analytical method that determines changes in weight in relation to change in temperature.

3.2 Materials

3.2.1 Polyamide 6

A polyamide 6 (PA6) under the trademark name of ZISAMIDE ®TP4210 and provided by Zig Sheng Industrial Co.Ltd (China). It widely used in many different market and applications due to their very good performance and cost ratio. Several parts are made with these PA6 in the transportation, packaging industries, electrical and electronics. Obviously, PA6 has a wide range of engineering application for its unique combination of good processibility, higher mechanical properties and chemical resistance.

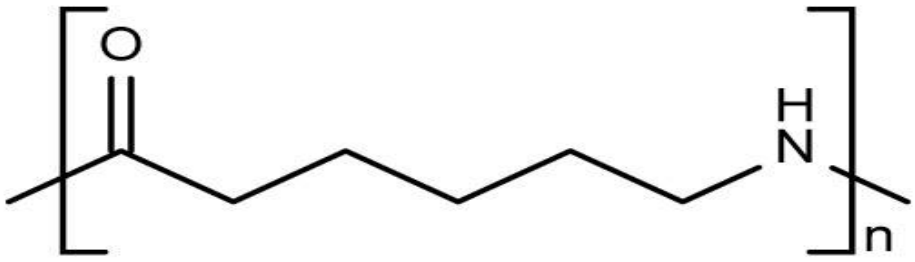

Figure 3.1: Chemical structure of PA6

(Source: Chavarria and Paul, 2004).

Table 3.1: Physical and Chemical properties of PA6

Physical and Chemical properties of PA6	
Physical state	solid
Form	granules
Colour	Undyed (from white to light yellow)
Odour	odourless
Specific gravity	1.14
Ignition temperature	min. 395°C
Melting point	(213 - 215) °C
% Volatiles by volume	21°C
Solubility in water	insoluble
Density at 20 °C	1130 kg/m3

3.2.2 Cloisite 20A

The Cloisite 20A (C20A) with chemical name of dimethyl dihydrogenatedtallow quaternary ammonium (2M2HT) is purchased from Southern Clay Products Inc., USA. The higher values of modifier concentration in C20A might works in both ways, as the increased number of organic components in the presence surfactant pushed the intergalleries separately and increased the thermal decomposition tempo of PA6/C20A due to the low thermal stability of alkyl ammonium tail. C20A also used as additives to enhance flexural and tensile modulus, barrier properties and flame retardancy of thermoplastics

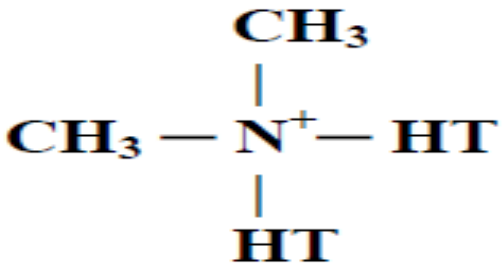

Figure 3.2: Chemical structure of C20A, where HT is Hydrogenated Tallow (~65% C18; ~30% C16; ~5% C14)

Table 3.2: Physical and Chemical properties of C20A

Physical and Chemical properties of C20A	
Physical state	solid
Form	Powder
Colour	Off-white
Odour	odourless
Specific gravity	1.4 - 1.8
Auto-ignition temperature	190 °C Thin Film Ignition
% Volatiles by volume	0 % estimated
Solubility in water	insoluble

Table 3.3: Materials designation code and composition PA6 and C20A

Condition	Temperature Profile	PA6 (wt %)	C20A (wt %)	Designation Code
Autothermal	Constant	100	0	Pure PA6
	Constant	99	1	PA6/C20A/1
	Ascending			PA6/C20A/1
	Descending			PA6/C20A/1
	Constant	97	3	PA6/C20A/3
	Constant	95	5	PA6/C20A/5
Conventional	Constant	100	0	Pure PA6
	Constant	99	1	PA6/C20A/1
	Ascending			PA6/C20A/1
	Descending			PA6/C20A/1
	Constant	97	3	PA6/C20A/3
	Constant	95	5	PA6/C20A/5

3.3 Preparation Of Fabricated PA6/C20A Nanocomposite

A compounding process of nanocomposite, which is according to **Table 3.3** were completed by simultaneously adding all the components to the PRISM EUROLAB 16 co-rotating-twin-screw extruder of dimension 1.5 x 7 x 1.5 m with 40:1 L/D see **Figure 3.3.** The PA6 and C20A were dried in the vacuum at 90°C respectively for 19 hour before hand in order to remove the water presence to avoid hydrolysis mechanism (Nawani et al., 2007). The PA6 nanocomposite is prepared in term of weight percentage and C20A is added between 1 – 5 % wt together with PA6 composite into the blends is determined as the table **Table 3.3**. The extruder was subjected to be operated under conventional initially, where this means that heating elements of extruder was allowed to be continuously switched-on during the melt-mixing of PA6/C20A.While for an

autothermal, the preheated plates were switched-off throughout the compounding process and only turned on back if the temperature was fallen almost to the minimum tolerance value (224± 5 °C).

The temperature segments of extruder were adjusted to three different set of temperature profile constant, ascending and descending, which range from 190°C to 224°C (Ray et al., 2002), while the die temperature was assigned at 200°C to ensure a better flow of extruded string of PA6/C20A nanocomposite from water bath. Set the maximal screw rotation speed at a rate of 200 rpm. This is followed by the extruded being pelletized by the Standard Granulator Fixed Length Pelletizer. All samples are allowed to ambient temperature for at least 48 hours prior to testing.

Figure 3.3: Twin Screw Extruder (PRISM EUROLAB 16)

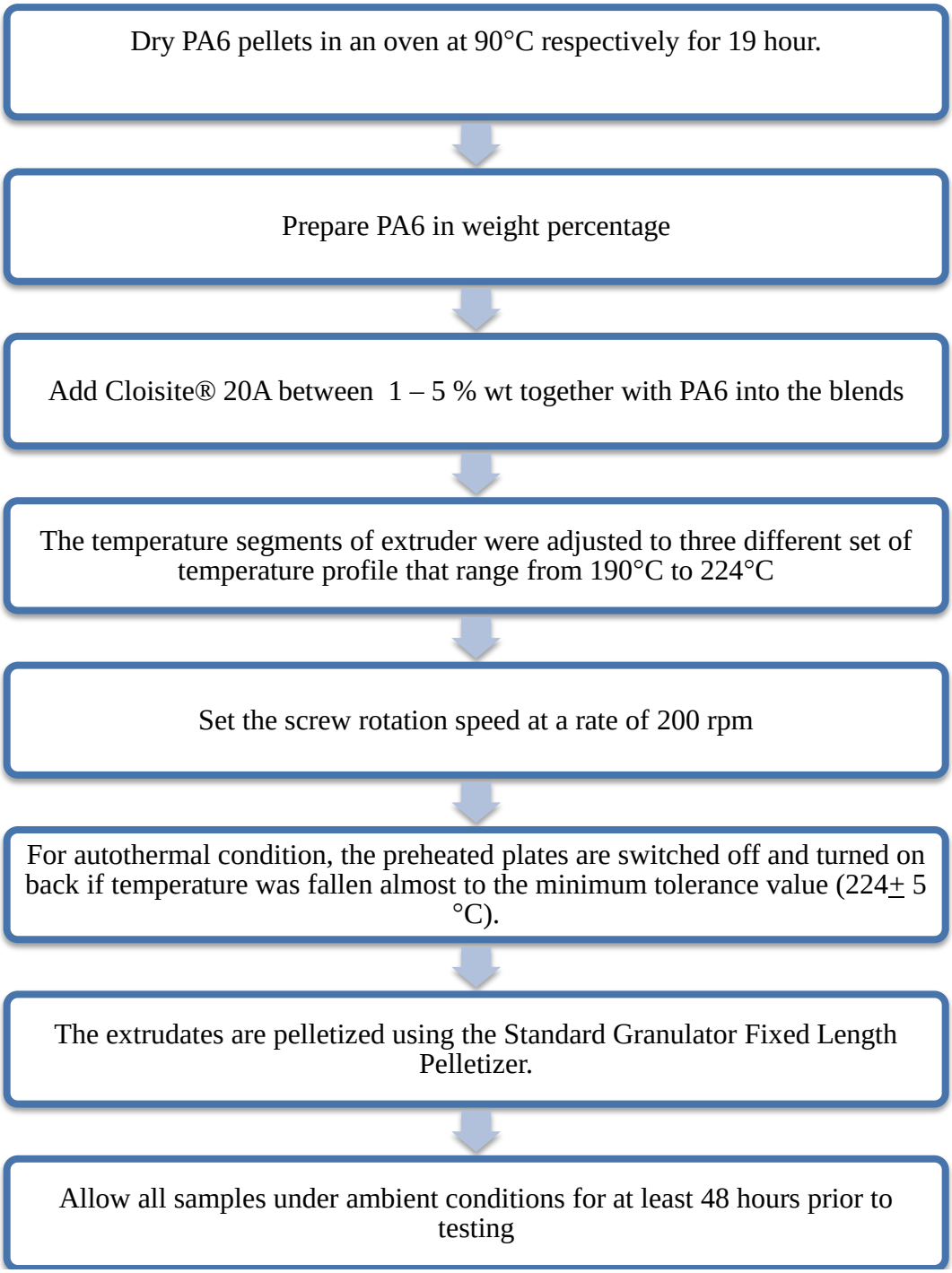

Figure 3.4: Preparation of Fabricated PA6/C20A Nanocomposite

3.4 Thermal Analysis

3.4.1 Thermo gravimetric Analysis (TGA)

TGA measure the amount and rate of change in the weight of material as a function of temperature or time in a controlled atmosphere. Measurement is used primarily to determine the composition of materials and predict their thermal stability at temperature up to 1000°C. The technique can characterize materials that exhibit weight loss or gain due to decomposition, oxidation or dehydration. Thus, the thermal stability of fabricated PA6/C20A nanocomposite was determined throughout the application of TGA by using TGA system (Mettler Toledo) see **Figure 3.5** under nitrogen (N_2) environments. By using this TGA method could be determines changes in weight in relation to change in temperature.

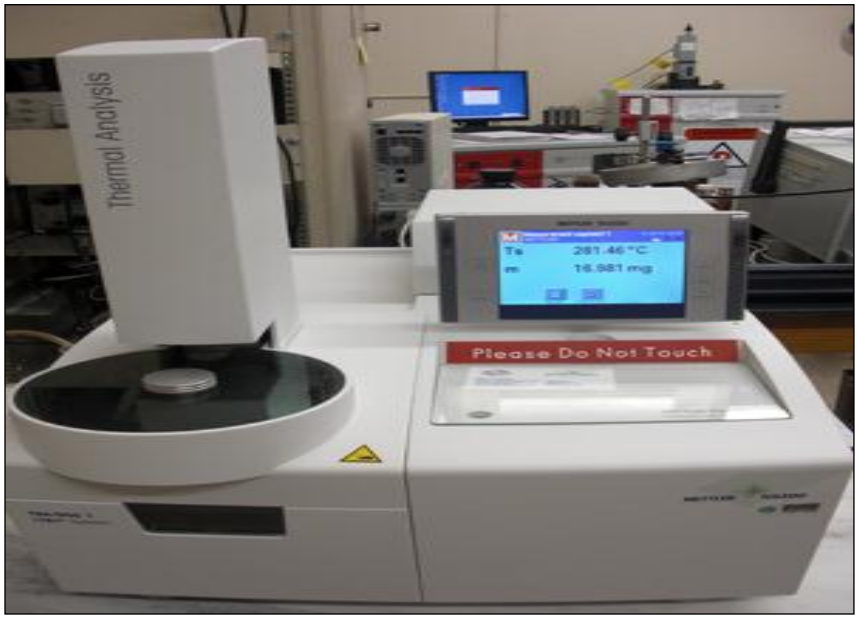

Figure 3.5: TGA system (Mettler Toledo)

A sample is loaded against a pan and place on the balance; the sample must be solid form only that ranges from 1- 6 mg. Then, heat the fabricated PA6/C20A nanocomposite from room temperature at a heating rate of 20°C min^{-1} under nitrogen atmosphere. Consequently, mass change versus temperature curve will provide the information of thermal stability for the samples by using STARE software in TGA system. Once test finish for the first sample, wait until the temperature 35°C and sample unloaded. Clean up the pan using ethanol solution and gas burner. Put the pan lid and click 'TARE' to measure weight pan combine with sample not more than <5mg.

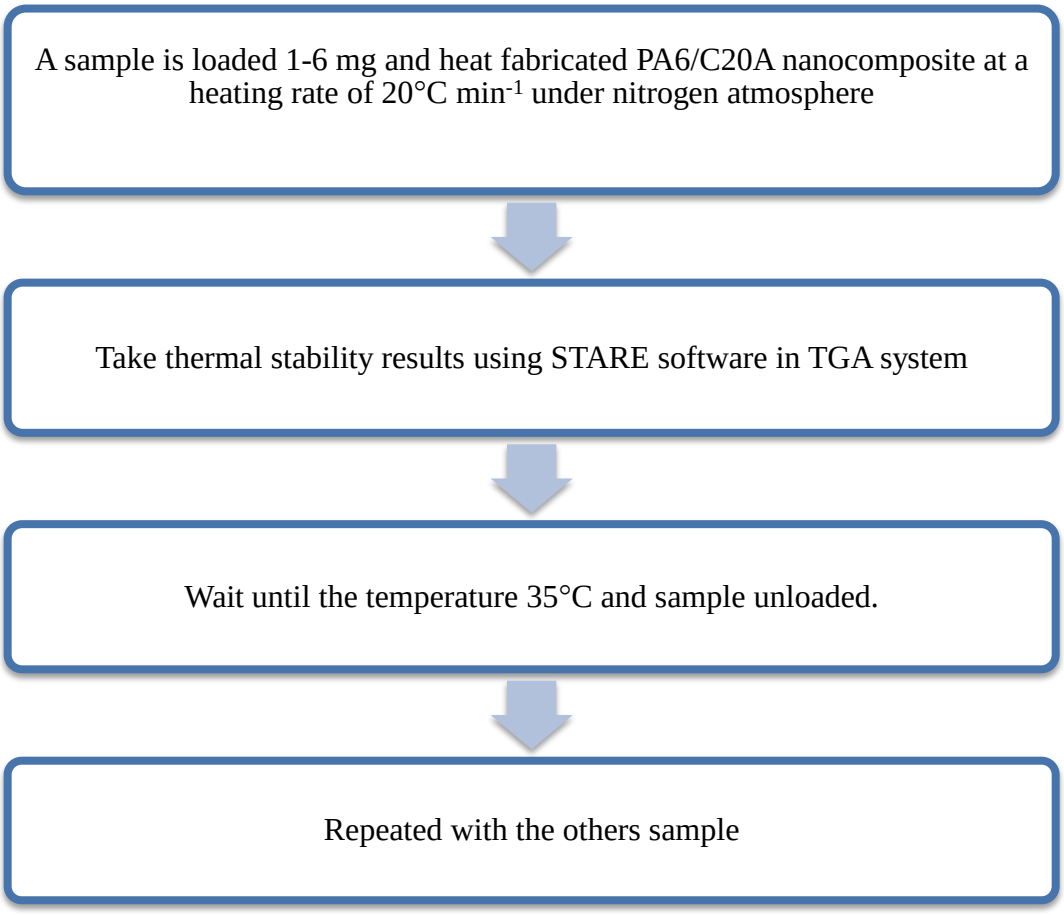

Figure 3.6 :Characterization method using TGA

3.5 Morphological Analysis

3.5.1 X-Ray Diffraction Analysis (XRD)

XRD is a non-destructive analytical technique which can yield the unique fingerprint of Bragg reflections associated with a crystal structure. XRD appropriate to ease and availability to morphology analysis. Thus, XRD can measure the average spacings between layers or rows of atoms and determine the orientation of a single crystal or grain. Besides that, it can measure the size, shape, internal stress of small crystalline regions and invention the crystal structure of unknown material.

The analysis is carry out by using XRD Miniflex II by Rigaku see **Figure 3.7**. This analytical tool probes the crystal lattice structure of the nanocomposite. An x-ray is projected into the sample.

$$d = \frac{n\,x}{2\,d \sin \emptyset} \qquad (1)$$

Where:

d = Space between layers of the clay

λ = Wavelength of the X-ray which is 0.154nm

θ = Angle at the maximum point of the first peak into spectrum

n = Order of diffraction

Figure 3.7: XRD Miniflex II by Rigaku

Accordingly to this analysis, a small amount of PA6/C20A nanocomposite sample was placed on the slot and the surface of the slot was in contact with that sample as shown in **Figure 3.8**. Then the sample and the slot were put into XRD machine. The samples are scanned in fixed step size, 0.02 with a step-time of 1s in the range of 3-10°. Based on the scanning, an XRD diffractogram (intensity 20) is obtained. Then, the d-spacing (d) of the interlayer gallery of Cloisite 20A and PA6 based nanocomposites is calculated using Bragg's Law equation (1) which it is the software system in the XRD Miniflex equipment. By varying the angle *theta* (θ), the Bragg's Law conditions are satisfied by different *d*-spacings in polycrystalline materials. Plotting the angular

positions and intensities of the resultant diffracted peaks of radiation produces a pattern, which is characteristic of the sample. Where a mixture of different phases is present, the resultant diffractogram is formed by addition of the individual patterns.

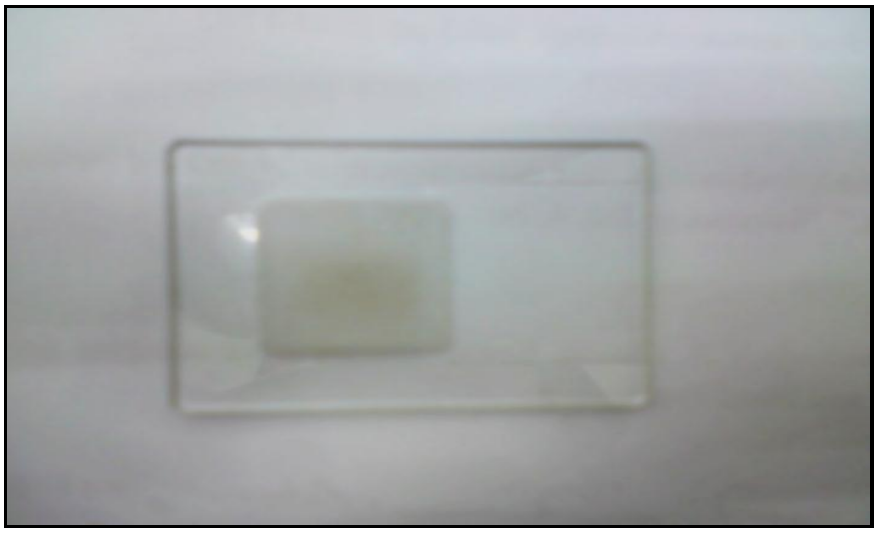

Figure 3.8: Sample on the slot

Based on the principle of X-ray diffraction, a wealth of structural, physical and chemical information about the material investigated can be obtained. A host of application techniques for various material classes is available, each revealing its own specific details of the sample studied.

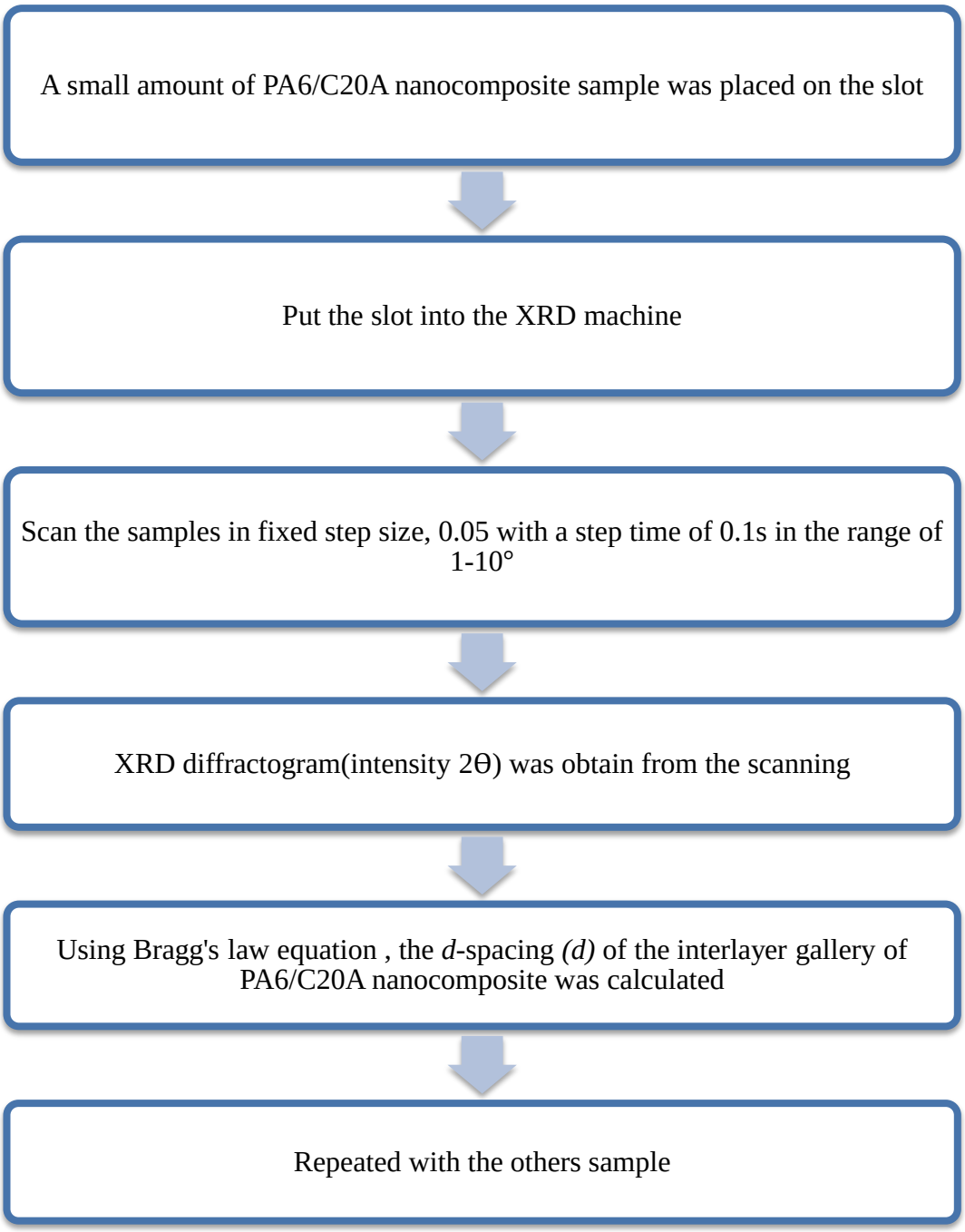

Figure 3.9: Characterization method using XRD

3.5.2 Scanning Electron Microscopy (SEM)

The SEM is a microscope that uses electrons instead of light to form an image. Furthermore, SEM has allowed researchers to observe a much bigger variety of specimens. The scanning electron microscope has many advantages over traditional microscopes. The SEM has a large depth of field, which allows more of a specimen to be in focus at one time. The SEM also has much higher resolution, so closely spaced specimens can be magnified at much higher levels (Chan et al., 2002). Because the SEM uses electromagnets rather than lenses, the researcher has much more control in the degree of magnification. All of these advantages, as well as the actual strikingly clear images, make the scanning electron microscope one of the most useful instruments in research today.

Hence the structure of nanocomposite has typically been established using SEM by ZEISS EVO50 see **Figure 3.10**, which observation to allow surface roughness and morphology dispersion degree of clay particles. Under this setup, carbon tape was pasted on the Stub. Stub is one of the equipment that involve in SEM analysis to put the sample as seen in **Figure 3.11**. Then, 3-4 granule of PA6/C20A nanocomposite was placed on the carbon tape. The Stub put into the coating machine (Platinum), which sample was coated with platinum to increase the conductivity. Next, the Stub was transferred to SEM chamber for SEM analysis (imaging process). Before run the experiment, the parameter was setup with its (EHT: 10kv, I probe: 100pA, WD: 8-9mm and Mag: 300x). Finally, the sample ready to analysis after SEM image appeared.

Figure 3.10: SEM by ZEISS EVO50

Figure 3.11: Carbon tape was pasted on the Stub

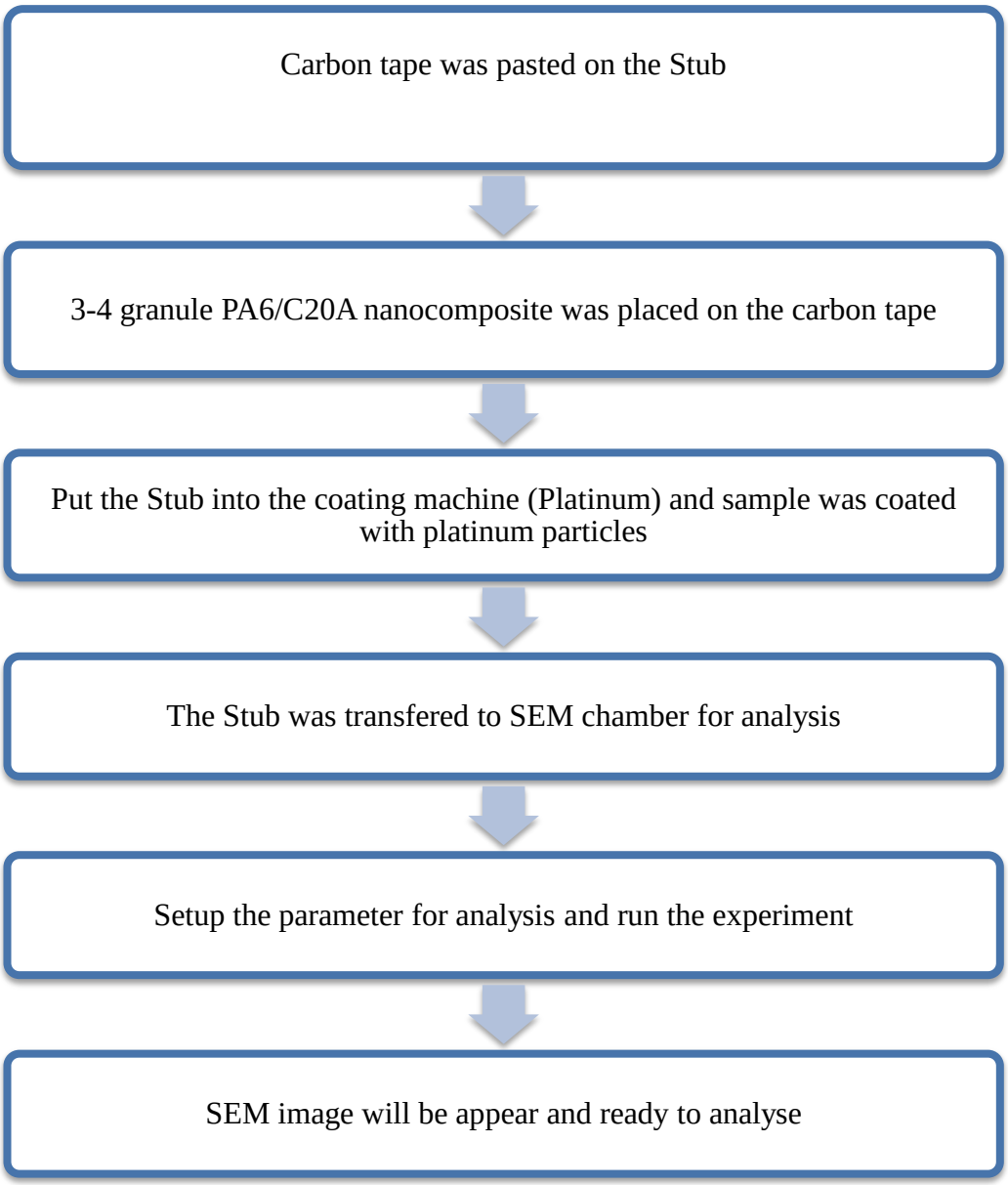

Figure 3.12: Characterization method using SEM

CHAPTER FOUR

RESULT & DISCUSSION

4.1 Thermal Analysis PA6/C20A nanocomposite using TGA

The thermal stability of PA6/C20A nanocomposite is usually studied by thermogravimetric analysis (TGA). The weight loss due to the formation of volatile products after degradation at high temperature is examined as a role of temperature. Thus, the thermal stability of fabricated PA6/C20A nanocomposite was determined throughout the application of TGA by using TGA system (Mettler Toledo). Generally, the incorporation of clay into the polymer matrix was found to enhance thermal stability by acting as a superior insulator and mass transport barrier to volatile products generated during decomposition. Recently, there have been many reports concerned with the improved thermal stability of nanocomposite prepared with various types of clays and polyamide (Sepe, 1997). Furthermore, combination of polymer and clay nanocomposite preparation involves high temperatures irrespective of the fabrication route. Uncertainly processing temperature is higher than the thermal stability of the organic, decomposition will take place, primary to

variations between the nanofiller and polymer. Therefore, value of the T_{Onset} of degradation, follow-on products of degradation and the stability of the polymer is critical (Fornes et al., 2003). As a conclusion, TGA is great technique for investigating the thermal degradation of polymer nanocomposite.

Accordingly, **Table 4.1** presents the TGA-analysis for time at which 10 wt.% and 20 wt.% losses as well as the onset degradation temperature, T_{Onset} for pure PA6 and PA6/C20A nanocomposites with different C20A loadings under auto thermal and conventional extrusion at 200 RPM. TGA was conducted under influence of nitrogen (N_2) environments. As can be seen in **Table 4.1**, the sample of conventional extruded PA6 with 1wt. % C20A displayed higher value of degradation T_{Onset} value at 405°C as compared to the auto thermal extruded PA6 with 5wt.% of C20A as the degaradation crept in at the temperature of 401°C.The thermal degradation for PA6 with 3wt% C20A and neat PA6 were found to be at the similar value of 406°C. The variation of the degradation temperatures at which 10 and 20wt% mass loss occurs for neat PA6 and C20A nanocomposites under auto thermal extrusion is shown in **Table 4.2**

Table 4.1: Conventional at 200rpm under $T_{constant}$

Clay content (%)	Time 10wt % (min)	Time 20wt % (min)	T 10wt % (°C)	T 20wt % (°C)	T Onset (°C)	T endset (°C)
0	72.62	76.54	392	410	406	465
1	72.82	76.8	395	408	405	465
3	71.97	76.05	390	407	406	460
5	72.3	75.93	389	405	401	460

Table 4.2: Auto thermal at 200rpm under $T_{constant}$

Clay content (%)	Time 10wt % (min)	Time 20wt % (min)	T 10wt % (°C)	T 20wt % (°C)	T Onset(°C)	T endset (°C)
0	72.92	77	391	409	406	467
1	72.37	76.52	390	408	407	463
3	72	75.82	389	404	399	461
5	71.8	75.22	382	402	400	456

It was found for PA6 with 1wt% C20A that the degradation T_{Onset} for sample that was collected under auto thermal extrusion was observed to be higher than degradation T_{Onset} of the conventional extrusion which valued at 407°C as agreed by (Fornes et al., 2003). However, the addition of higher C20A content (3wt. % and 5wt. %) into the matrix of PA6 did decrease the resistance of PA6/C20A nanocomposite against the thermal degradation $T_{Onset.}$. This observation might be correlated with the amount of clay content used as proved by **Figure 4.8** from SEM characterization.

Table 4.3: Conventional at 200rpm with various types of $T_{profile}$ with 1 wt. % C20A.

Tprofie(°C)	Time 10wt % (min)	Time 20wt % (min)	T 10wt % (°C)	T 20wt % (°C)	T Onset (°C)	T endset (°C)
Constant	72.82	76.8	395	408	410	465
Ascending	72.45	76.92	391	412	406	461
Descending	72.37	76.43	385	406	405	462

Table 4.4: Auto thermal at 200rpm with various types of $T_{profile}$ with 1 wt. % C20A.

T profie(°C)	Time 10wt % (min)	Time 20wt % (min)	T 10wt % (°C)	T 20wt % (°C)	T Onset (°C)	T endset (°C)
Constant	72.37	76.52	390	408	406	463
Ascending	72.62	76.45	389	410	407	463
Descending	72.75	76.65	388	407	407	465

Additionally, the TGA-analysis for time at which 10 wt.% and 20 wt.% losses as well as the onset degradation temperature, T_{Onset} for pure PA6 and PA6/C20A nanocomposites with different extruder temperature profiles are summarized in **Table 4.3** and **Table 4.4.** There are three types of $T_{Profile}$ that were used during this research, constant, ascending and descending. The descending $T_{Profile}$ of extruder produced sample with the highest T_{Onset} value at 405°C and 407°C respectively for both of extrusion system conventional and auto thermal as agreed by Rao et al (1981). Oppositely, the T_{Onset} for degradation is lower in value for PA6/C20A nanocomposite with ascending $T_{Profile}$ where the thermal degradation crept in just at the temperature of 406°C for conventional extrusion and 407°C for auto thermal extrusion.

Figure 4.1 represents the TGA analysis of auto thermal nanocomposite compared with conventional nanocomposite. This graph is the function of value of T_{Onset} and clay loading at screw speed 200 rpm with the constant temperature extruder profile and varied clay loading (1wt. %, 3wt. % and 5wt. %). The addition of clay C20A at 1 wt.% under auto thermal extrusion interestingly increased the value of T_{Onset} as compared to the pure PA6,while the addition of similar amount of nano-scaled filler C20A under conventional extrusion reduced the value of T_{Onset}. Even

with 1 wt. % of clay loading in the nanocomposite, the value of T_{Onset} was significantly increased as agreed by Pramoda et al. (2003). The difference of T_{Onset} for 1 wt. %, 3wt. % and 5wt. % $_{was}$ related to the amount of silicate char formed in PA6/C20A nanocomposite. This char was act as barrier against heat and at 1 wt. % of clay loading in the nanocomposite would cover most of the area due to the exfoliation of clay layers in the PA6 matrix. The exfoliation of C20A clay at 1wt. % of clay loading in the matrices was proved from the XRD reading as shown in **Figure 4.5.** The SEM micrographs from **Figure 4.7** also visually support the exfoliated state of clay if based from the number of visible agglomerated/aggregated C20A clay. The increased value of T_{Onset} at 5 wt. % clay loadings in **Figure 4.1** might be caused by the larger presence of clay content in PA6 as compared to the 3 wt% of clay loading. As a result, larger area could be covered by silicate char formation during the heating as this char later would act as a barrier against heat diffusion in the matrix, which explains the better value of T_{Onset} at 5 wt. % clay loadings. The exfoliation of C20A clay at 5wt. % of clay loading in the matrices was also proved from the XRD reading as shown in **Figure 4.5.** The SEM micrographs from **Figure 4.8** also visually support the exfoliated state of clay if based from the number of visible agglomerated/aggregated C20A clay.

Besides that, the agglomeration/aggregation of C20A clay was cited as a factor that led to this type of reading since only an exfoliated morphological structure of PA6/C20A possessed an ability to enhance the thermal stability of a material. Liu et al. (2002) was agreed that the morphological observations that show only exfoliated polymer nanocomposites exhibit improved thermal stability. While agglomerated clay particles do not significantly affect the thermal stability of the

polymer matrix. Thus, the advantageous influence of clay loading on thermal stability of polymers clearly depends on the degree of intercalation or exfoliation of clay layers. The better dispersion of nanofiller is achieved as same studies by Liu et al. (2002).

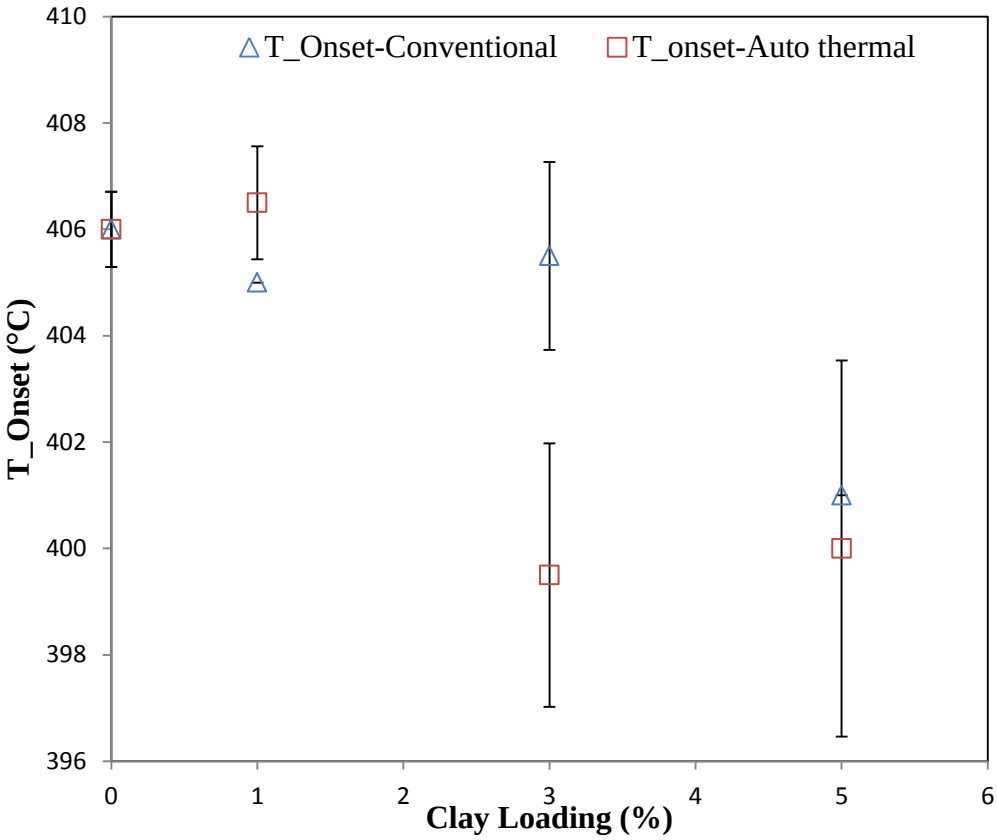

Figure 4.1 : Comparison of T_{Onset} of Auto thermal/Conventional at 200 rpm/$T_{Constant}$

On the other hand, Pramoda et al. (2003) also presented that the difference of the degradation temperatures at which 5 and 10 wt. % loss occurs for neat PA6 nanocomposites as shown in **Figure 4.2**. The T_{Onset} for degradation was found to be 12°C higher for nanocomposite with 2.5 wt. % clay addition than that for neat PA6. This shows that PA6 nanocomposite with 2.5 wt. % of clay loading has greater thermal stability than the neat PA6 nanocomposite. This observation highlighted the

positive influence of clay on the thermal resistant property of PA6/C20A nanocomposites. However, a further addition of clay C20A into the PA6 that up to 5 wt. % did not increase the value of T_{Onset} but in contrast weakened the thermal resistant of PA6/C20A nanocomposite against heat under N_2 atmosphere. Both of conventional and auto thermal extrusion system demonstrate a similar trend as shown in the **Figure 4.1**.

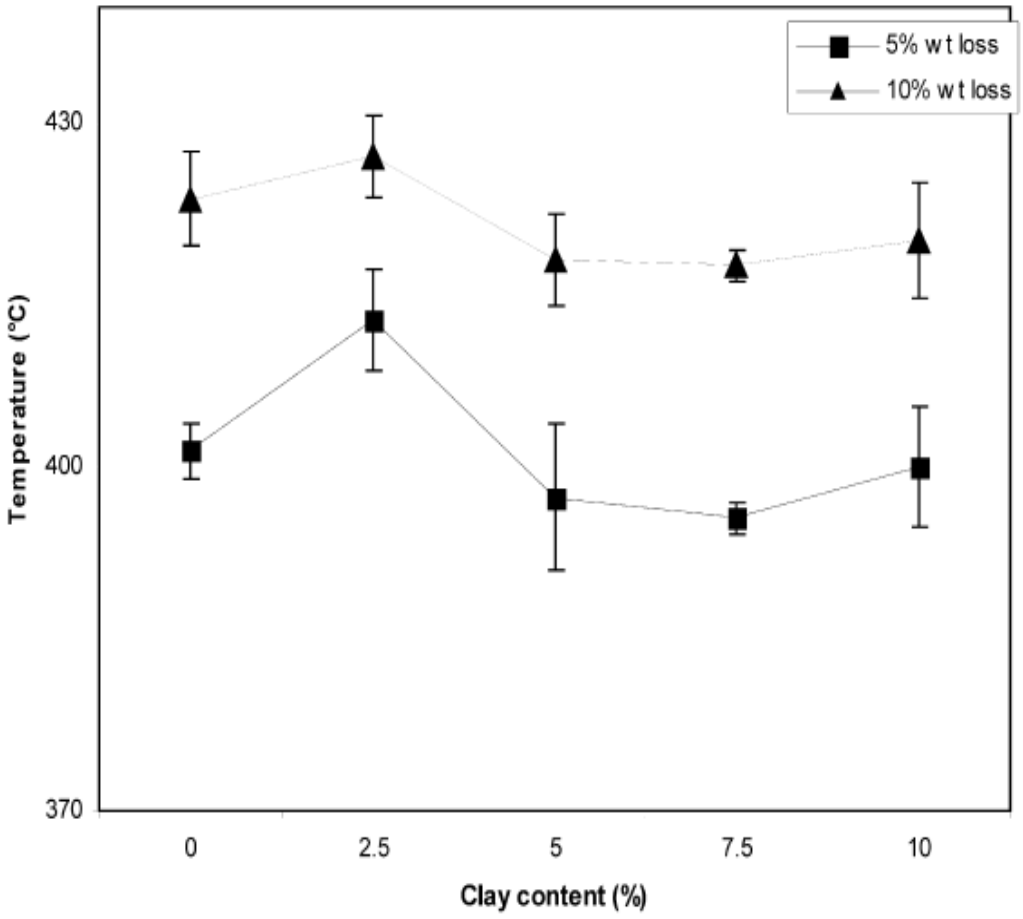

Figure 4.2: The 5 and 10wt% loss temperature function of clay loading (wt%) (Source: Pramoda et al., 2003).

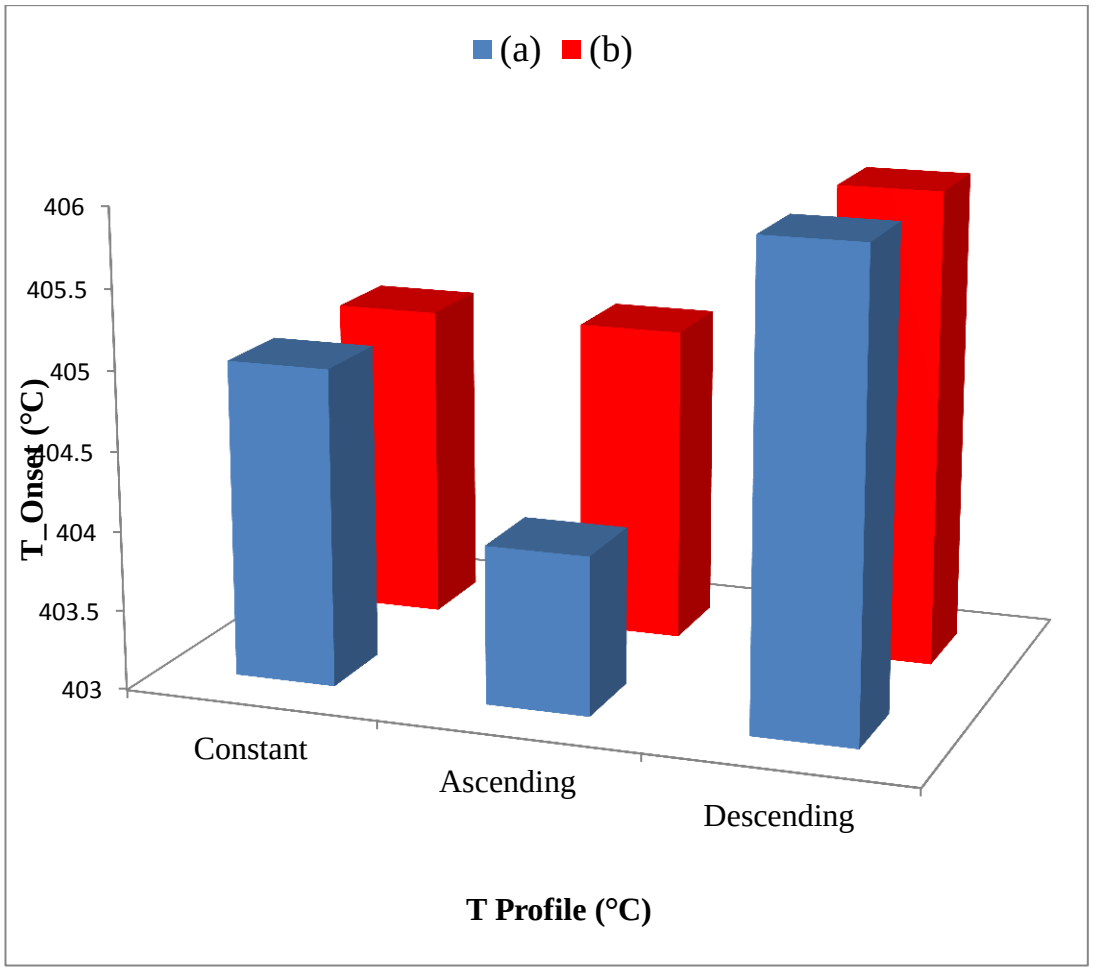

Figure 4.3: Function of T_{Onset} and $T_{Profile}$ at speed 200 rpm with 1 wt. % C20A. (a) T_{Onset} Conventional (b) T_{Onset} Auto thermal

The **Figure 4.3** aboved shows the function of T_{Onset} and three types of $T_{Profile}$ of extruder, at screw speed of 200 rpm and 1 wt. % of C20A. The descending temperature profile of extruder, $T_{Profile}$ produced sample with the highest T_{Onset} value for both of extrusion system conventional or auto thermal. The higher temperature zone at feeding area increased the rate of melting for PA6 pellet as lower temperature zone was required at homogenizing zone due to the presence of organic component in the clay C20A, which require low heat energy due to the sensitivity of organic component to heat (Rao et al, 1981). As a result, the risk of thermal

degradation was reduced and thermal stability of PA6/C20A nanocomposite was enhanced due to the presence of clay C20A in the PA6 matrix (Pramoda et al., 2003). In contrast, the ascending temperature profile of extruder, $T_{Profile}$ formed sample with the lowest T_{Onset} value under conventional extrusion. The lower temperature zone at feeding area decreased the rate of melting for PA6 pellet while high temperature zone in the homogenizing area increased the rate of thermal degradation of organic component in the clay C20A (Crowley, 2007). Consequently, the value of T_{Onset} was not increased as expected.

Besides that, it is interestingly to point out that auto thermal extrusion system successfully reduced the risk of thermal degradation for the C20A clay under setting of ascending temperature profile, as the T_{Onset} visibly influenced a similar value to the T_{Onset} of constant temperature profile of extruder. The lack of heat energy supplied from heating element of extruder did not influence the quality of PA6/C20A nanocomposite in a negative way as the mechanical energy from screw speed of extruder was converted into heat energy in the form of viscous heat that distributed throughout of molten compound (Vaia et al, .1996).

4.2 Dispersion of PA6/C20A nanocomposite using XRD

XRD is a non-destructive analytical technique which can yield the unique fingerprint of Bragg reflections associated with a crystal structure. XRD appropriate to ease and availability to morphology analysis. Thus, XRD can measure the average spacing between layers or rows of atoms and determine the orientation of a single

crystal or grain. Besides that, it can measure the size, shape, internal stress of small crystalline regions and invention the crystal structure of unknown material. The analysis is carry out by using XRD Miniflex II by Rigaku

The morphology of PA6 composites with clay loading higher than 10 wt. % was only described by Shah and Paul (2004) for masters of high molecular weight PA6 with an organoclay modified with octadecyltrimethyl ammonium ions. The XRD arrangements of the melt-compounded PA6 composites containing clay loading 0, 5, 10, and 20 wt. % of cloisite 30B are presented in **Figure 4.4.** However, the composite with 20 wt. % 30B suggesting the presence of intercalated tactoids with $d_{0\,0\,1} \approx 3.7$ nm. The appearance of this reflection can be interpreted considering that, during the slow illustration cycle of this sample, the silicate lamellae were separated in the formless regions, thus making their concentration increase considerably, above the average value, so that their aggregation to form intercalated stacks was favored. Intercalation at high MMT loadings for nanocomposites of an amorphous polyamide with an organoclay modified with dimethyl benzyl hydrogenated tallow ammonium ions (Zhang, 2009). An intercalated structure with $d_{0\,0\,1} = 3.68$ nm for nanocomposites of PA6 containing more than 10 wt. % of an organoclay modified with octadecyl ammonium cations (Liu et al., 2002). Since only an exfoliated morphological structure with the decrease clay loading have the value of 2Ɵ as well as the peak is shifted towards a bigger angle compared to intercalated structure is obtained a smaller angle.

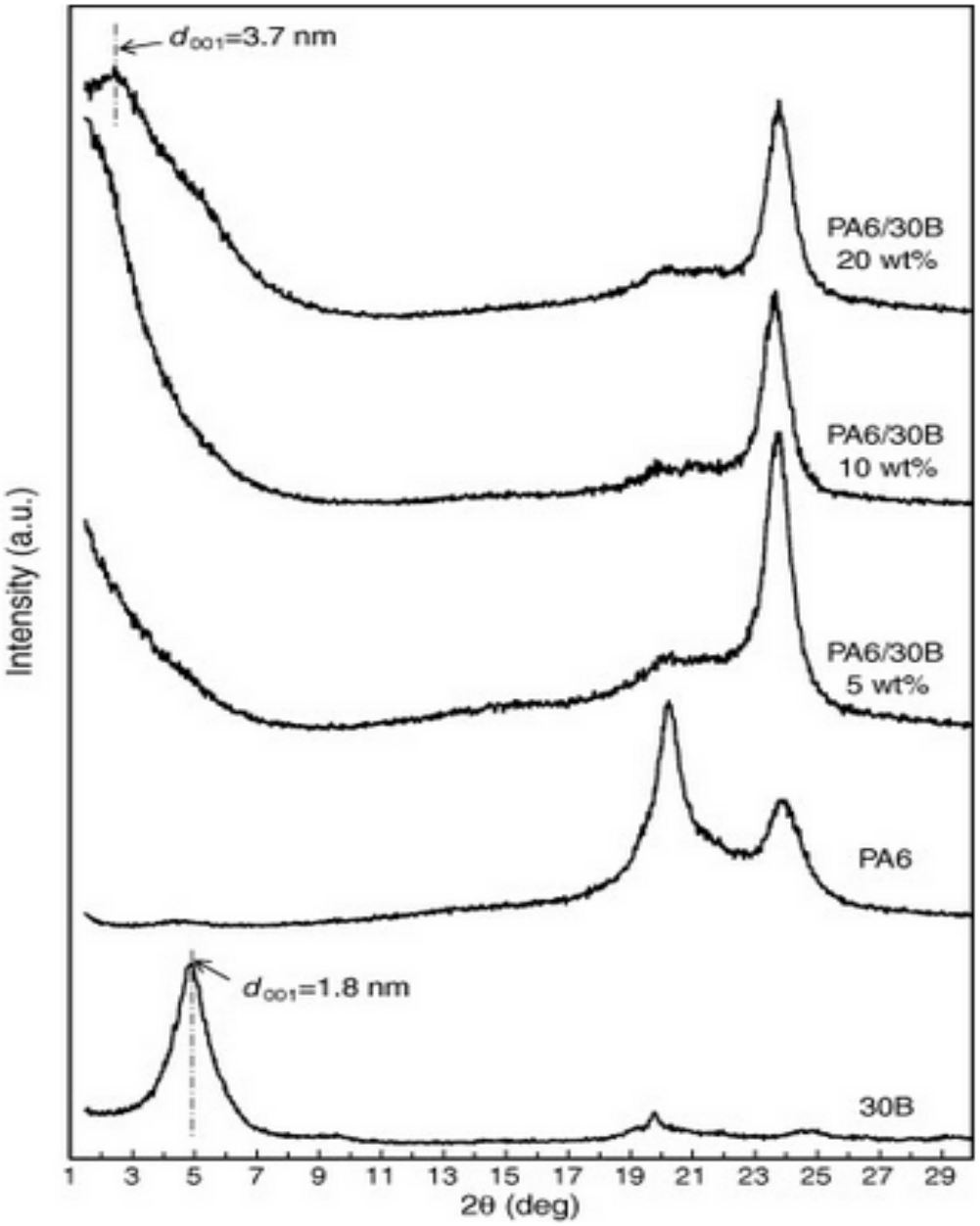

Figure 4.4: XRD patterns of 30B and melt-compounded PA6/30B composites sample with 0, 5, 10 and 20 wt. % clay

(Source: Shah and Paul, 2004)

Throughout the samples analysis by XRD, Lee (2003) has mentioned that an intercalated structure is obtained if the value of 2Θ as well as the peak is shifted towards a smaller angle. Additionally, for an exfoliated structure of nanoclays

platelets where the absence of peak is supposed to be synchronized with the exfoliation feature, as an exfoliated tactoids should influenced a gallery space that is more than 8.8 nm (Utrucki, 2004) greater than the XRD device could measure. In the **Figure 4.5**, shows the curves of PA6/C20A nanocomposite that were obtained from XRD analysis mainly for a comparison purpose. Each of the curves was labeled and plotted with different color to distinguish between conventional or auto thermal extrusion and varied clay loading (1-5 wt. %).

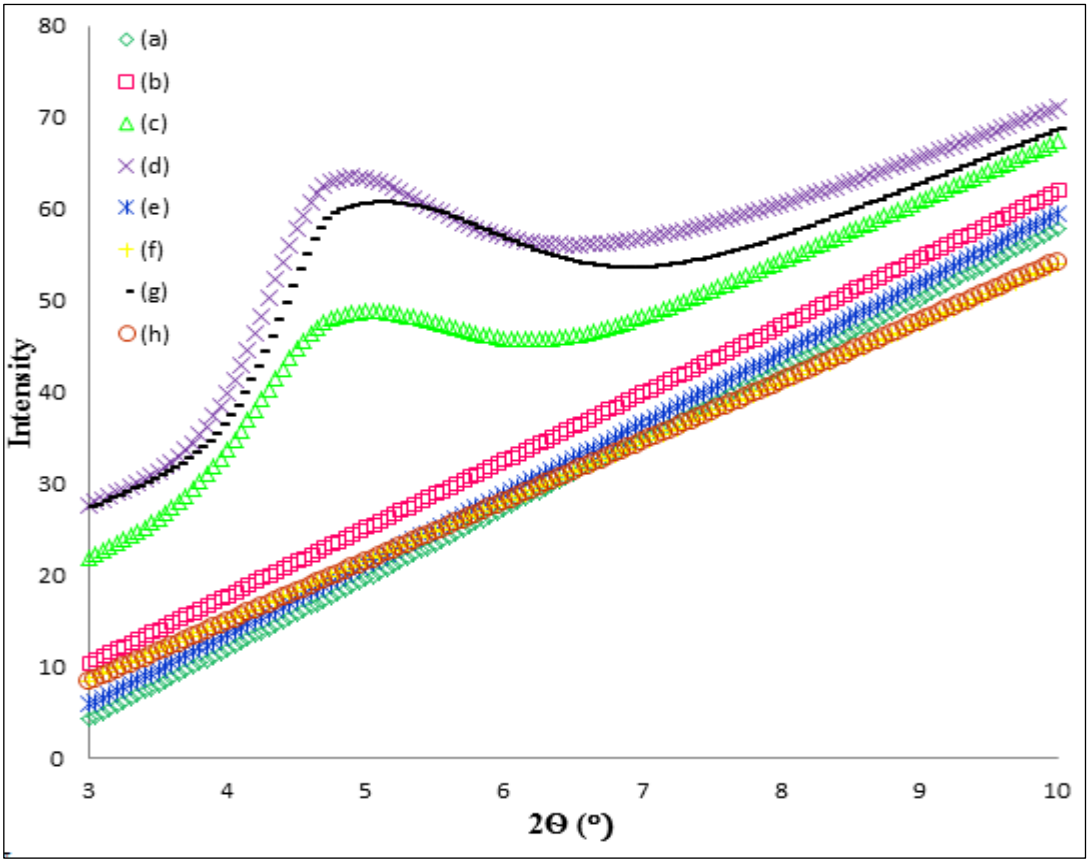

Figure 4.5 : $T_{constant}$ with various clay loading at speed 200rpm. Auto thermal (a)PA6/C20A (b)PA6/C20A/1 (c)PA6/C20A/3 (d)PA6/C20A/5, Conventional (e)PA6/C20A (f)PA6/C20A/3 (g)PA6/C20A/5 (h)PA6/C20A/1

Figure 4.5 representes the auto thermal and conventional at speed 200 rpm under $T_{constant}$ with various clay loading. Moreover, at zero and 1 wt. % of C20A

loading in PA6, there was no visible peak that could be observed in the diffractograms. However at 3 wt. % of C20A, the curve for auto thermal extruded sample shown a presence of peak at 2θ = 4.73° that hinted at the possibly of intercalated structure. There was no peak was observed for the conventional extruded sample. While, at 5 wt. % of C20A, both of conventional and auto thermal extruded curves possessed a visible peak at 2θ = 4.74° for auto thermal compounding and 2θ = 4.77° for conventional extrusion respectively. The increased amount of clay was cited as factor that led to the aggregation/agglomeration in the PA6 due to the lack of shear stress/strain supplied by the mechanical energy of extruder as an agreed by Liu et al. (2002).

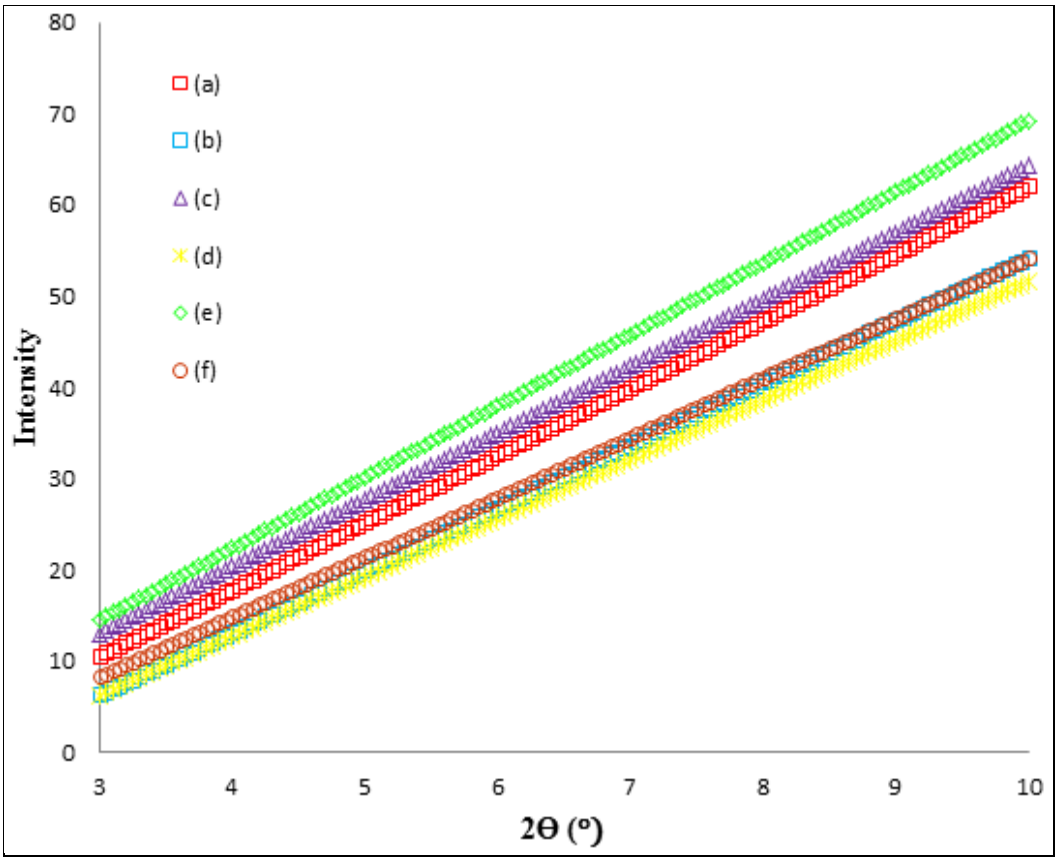

Figure 4.6: Various types of $T_{Profile}$ with clay loading 1 wt. % C20A at speed 200rpm. Auto thermal (a) PA6/C20A/1 constant (b) PA6/C20A/1ascending (c) PA6/C20A/1 descending, Conventional (d) PA6/C20A/1 ascending (e) PA6/C20A/1 descending (f) PA6/C20A/1constant

Figure 4.6 represents auto thermal and conventional extrusion at 200 rpm with various $T_{Profile}$ /1 wt. % C20A. On this graph, all the curves there were no visible peak that could be observed in the diffractograms. This observation conclusively, might lead to suggestion that a poor exfoliation of C20A platelets were took place here. In general, temperature profile did not affect the dispersion behavior of clay C20A in PA6 matrix (Vaia et al, .1996).

4.3 Morphology of PA6/C20A nanocomposite using SEM

The SEM is is a microscope that uses electrons instead of light to form an image. SEM has allowed researchers to observe a much bigger variety of specimens. The scanning electron microscope has many advantages over traditional microscopes. The SEM has a large depth of field, which allows more of a specimen to be in focus at one time. The SEM also has much higher resolution, so closely spaced specimens can be magnified at much higher levels (Chan et al., 2002). Because the SEM uses electromagnets rather than lenses, the researcher has much more control in the degree of magnification. All of these advantages, as well as the actual strikingly clear images, make the scanning electron microscope one of the most useful instruments in research today.

In general, a quality of dispersion and distribution of delaminated platelets in the polymer matrix were comparatively associated to the amount clay content used as showed by the SEM. **Figure 4.7** and **4.8** representing the results of SEM patterns of various nanocomposite samples at 300x magnification as each of the sample

contained 1wt. % and 5wt. % of C20A loading under auto thermal and conventional system. The presences of objects of sizes within 20μm were observed. While each of the samples demonstrated presence of agglomerates in the matrices, the number and dimension of visible agglomerates were varying. The number of the aggregate slightly decreases and the size was small during sample 1wt. % of clay loading. As compared to the sample 5wt. % of clay loading that featured medium amounts of aggregate as well as the size were bigger (Pramoda et al., 2003)

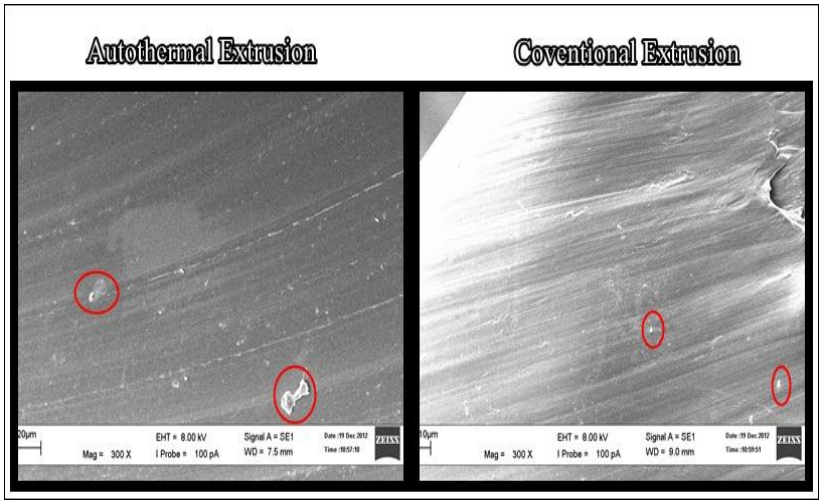

Figure 4.7: Auto thermal/ Conventional with Clay loading 1wt%+PA6

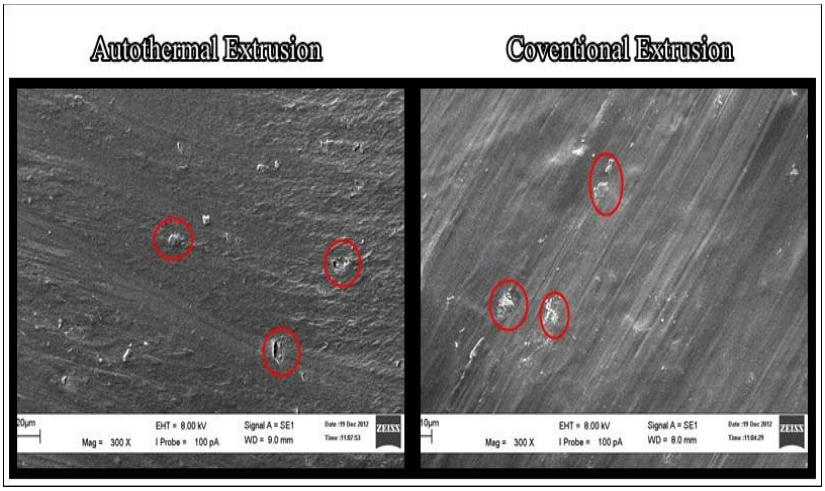

Figure 4.8: Auto thermal/ Conventional with Clay loading 5wt%+PA6

This morphology analysis for the sample contained 1wt. % and 5wt. % of C20A loading under auto thermal and conventional system were dependable with dispersion of PA6/C20A nanocomposite using XRD as shown in **Figure 4.5.** Based on the XRD diffractograms as the nonappearance of any basal reflection proved that the once orderly structured of clay loading has been previously disrupted by the shear forces originated from the rotation of twin screw extruder.

The sample dispersion and distribution quality is determined to be not good if it has more or large number of aggregate. The amounts of agglomeration and aggregation clay were not affected by the different of extrusion system; auto thermal or conventional. The increased clay content made it more difficult for the extruder to disperse it in the PA6 matrix (Vaia et al, .1996).

CHAPTER FIVE

CONCLUSION & RECOMMENDATION

5.1 CONCLUSION

This research is to study on the effect of C20A under conventional and auto thermal extrusion to the morphology structure and thermal stability of fabricated PA6/C20A nanocomposite.

In discussing the dispersion and distribution of nanoclays platelets within the polymer matrix, a clay contents show a better role in dictating the quality of extruded PA6/C20A nanocomposite than the auto thermal or conventional setting extruder if based from the number of agglomerated clay in PA6 matrix during the SEM observation. The degradation T_{onset} of PA6/C20A nanocomposite was found to be shifted to the larger value under an auto thermal extrusion. As a conclusion, auto thermal extrusion is suggested as an alternative approach to reduce thermal degradation of heat in the melt compounding method of PNC.

5.2 RECOMMENDATION

As a recommendation, it is suggested that extruder machine in the laboratory should be regularly being serviced by the technician. An experiment that involves lab extruder cannot be carried out and delayed if the machine is damaged due to the improper maintenance. It is important to ensure that only dry material is entered the extruder system during the melt operation. The presence of water or other small molecules provokes the hydrolytic chain scission of these nanocomposites with severe reduction of molecular weight and consequent deterioration of the final properties. In order to reduce the risk of degradation by hydrolytic chain scission in the compounded PNC, humidity and oxygen need to be removed from the extruder system during processing (Breyer et al., 1996). As a result, the processing of PA6/C20A nanocomposite would be easier and materials with unchanged properties could only be obtained if a careful drying step is carried out before the melt operation.

Besides that, it is suggested that combination of PA6 with Cloisite 30B (C30B) is better than C20A because C30B has an excellent exfoliation using twin screw extruder. A good PA6/C30B nanocomposite will be slightly amber in color and transparent, especially at extruder die (Crowley, 2007).

REFERENCES

Alexandre,D.P. (2000). Polymer layered silicate nanocomposites preparation, properties and uses of a new class of materials. *"Material Science Engineering,* Bd. 28, pp. 1-63

Aranda,P and Ruiz,H.E. (1992). Poly (ethylene oxide)-silicate intercalation materials. *Chem Mater 4*, pp. 1395–403

Bawa,R., Maebius,S.B., Flynn,T., Wei,C. (2005). Protecting new ideas and inventions in nanomedicine with patents. *Nanomedicine* 1, pp. 150-158.

Bernhardt,E.C. and McKelvey,J.hI. (1954). Presented at the 10th Annual Technical Conference of the Society of Plastics Engineers. *Toronto, Can.*

Beyer,G. (2002). Nanocomposites: a new class of flame retardants for polymers, "Plast *Addit Compound'.* Bd. 4, Nr. 10, pp. 22-27

Breyer,K., Regel,K., Michaeli,W. (1996). Polymer Recycling. Bd 2, pp. 251

Biswas,M. and Ray,S.S. (2001). Recent progress in synthesis and evaluation of polymer–montmorillonite nanocomposites. *Adv Polym Sci*.155, pp. 167–221.

Boisseau,P. and Zhang,L. (2011). Nano medicine: Nanotechnology in Medicine, " *Nanoscience and nanotechnologies: hopes and concerns.* Bd. 12, Nr. 7, pp. 620-636

Chan,C.M., Wu,J., Li,J., Cheung,Y. (2002). Polypropylene/calcium carbonate nanocomposite. *Polymer 43*, pp. 2981-2992.

Chin,I., Albrecht,T., Kim,H., Russell,T.P., Wang,J. (2001). On exfoliation of montmorillonite in epoxy. *Polymer 42*, pp. 5947-5952.

Chavarria,F., and Paul, D.R. (2004). Comparison of nanocomposites based on nylon6 and nylon 66. *Polymer 45*, pp. 8501-8515.

Clarke,A.R. (2002). Microscopy techniques for materials science. *CRC Press (electronic resource)*

Crowley, M.M. (2007). Pharmaceutical applications of hot melt extrusion: part I, 'Drug Development and Industrial Pharmacy'. Bd. 33, pp. 909-926

Denault,J. and Labrecque,B. (2004). Technology Group on Polymer Nanocomposites PNC-Tech.Industrial Materials Institute. National Research Council Canada. *75 de Mortagne Blvd. Boucherville,Québec, J4B 6Y4.*

Fischer,H. (2003). Polymer nanocomposites: from fundamental research to specific applications. *Materials Science and Engineering C* 23. pp. 763–772.

Fornes,T.D., Yoon,P.J., Keskkula,H., Paul,D.R. (2001). Nylon6 nanocomposites: the effect of matrix molecular weight. *Polymer 42*, pp. 9929–9940

Fornes,T.D., Paul,D.R., Yoon,P.J. (2003). Polymer matrix degradation and color formation in melt processed nylon 6/clay nanocomposites. *Polymer*, Nr. 44, pp. 7545-7556

Giannelis,E.P., Vaia,R.A., Ishii,H. (1993). Synthesis and properties of two-dimensional nanostructures by direct intercalation of polymer melts in layered silicates. *Chem Mater*

Greenland,D. (1963). Adsorption of polyvinyl alcohols by montmorillonite. *Journal Colloid Science.* Bd. 18, Nr. 7, pp. 647-664

Goos,S.C., Gonclaves,M.C., Felisberti. (1999). Journal of applied Polymer Science. Pp.72

James,M.M. (1954). Theory of Adiabatic Extruder Operation. *Industrial and Engineering Chemistr.*, Bd. 46, Nr. 4, pp. 5

Jordan,J., Jacobb,K., Tannenbaumc,R., Sharafb,M., Jasiukd, I. (2005). Experimental trends in polymer nanocomposites. *Materials Science and Engineering A.* pp.393:1–11.

Kojima,Y., Usuki,A., Kawasumi,M., Okada,A., Fukushima,Y., Kurauchi,T., Kamigato, O. (1993). Synthesis of nylon 6-clay hybrid. *Journal of Materials Research 8* . pp. 1185

Kolter,K. (2010). Hot-Melt Extrusion with BASF Pharma Polymers. *BASF Chemical Company.*

Krishnamachari,P., Zhang,J., Lou,J., Yan,J., Uitenham, L. (2009). A study of morphological, thermal and mechanical properties.

Kubies,D., Pantoustier,N., Dubois,P., Rulmont,A., Jerome,R. (2002). Controlled ring-opening polymerization of epsilon-caprolactone in the presence of layered silicates and formation of nanocomposites. *Macromolecules.* vol. 35, no. 9, pp. 3318-3320

Kudyakov,I.V., David,Z.R., Turro,N.J. (2009). Polyurethane nanocomposite

Lee,W., Choy,J.H., Kanatzidis, M.G., Wei,L., Rocci,L.M., Brazis,P., Kanneworf,C.R., Kim,Y.I. (2000). RuCl3/ Polymer nanocomposite: the first group of intercalative nanocomposite with transition metal halides. *Journal Am Chem Soc*

Lee,K.M. (2003). Effect of hydrogen bonding on the rheology of polycarbonate/organoclay nanocomposite. *Polymer*, vol.44, pp. 4573-4588

Lebaron,P.C., Wang,Z., Pinnavaia,T.J. (1999). Polymer-layered silicate nanocomposite: an overview. *Appl Clay Sci; 15*. pp. 11-29

Liu,Z.H., Liu,T.X., He,C.B., Sue,H.J., Yee,A.F. (2002). CS national meeting, *Orlando, USA*

McNally,T. (2003). Polyamide-12 layered silicate nanocomposite by melt blending, *Polymer*. Bd.44, pp. 2761-2772

McKelvey,J.M. (1962). Polymer processing. *Wiley, NY*

Mohanty,S., Nayak,S.K. (2007). Mechanical, thermal and viscoelastic behavior of nylon 6/clay nanocomposites with cotreated montmorillonites, *Polym -Plast. Technol. Eng.,* vol.46, pp. 367–376.

Morgan,A.B. and Gilman,J.W. (2003). Characterization of poly-layered silicate (clay) nanocomposite by transmission electron microscopy and X-ray diffraction, a comparative study. *Journal Application Polymer Science*

Nawani,P., Gelfer,M.Y., Hsiao,S.B, Frenkel,A., Gilman,J.W., Khalid,S. (2007). Surface modification of nanoclays by catalytically active transition. *Langmuir*. pp. 9808-9815.

Nina,N. (2002). Auto applications drive commercialization of nanocomposites, polymer additives colors. Retrieved from www.specialchem4polymers.com

Okada,A., Kawasumi,M., Usuki,A., Kojima,Y., Kurauchi,T., Kamigaito,O. (1990). Synthesis and properties of nylon-6/clay hybrids. In: *Schaefer DW, Mark JE, editor*. Polymer-based molecular composites. MRS Symposium Proceedings, Pittsburgh, vol. 171. pp. 45-50.

Powel,C.E., Beall,G.W. (2006). Physical Properties of Polymer/clay Nanocomposite. *Current Opinion in Solid State and Materials Science* 10. pp. 73-80

Pramoda,K.P., Liu,T., Liu,Z., He,C., Sue,H.J. (2003). Thermal degradation behavior of polyamide 6/clay nanocomposites. *Polymer degradation and stability 81*. Pp. 47-56

Rao,N.S. (1981). Designing machines and dies for polymer processing with computer programs. *Carl Hanser Verlag, Munich.*

Ray,S.S., Okamoto,M., Maiti,P., Yamada,K., Ueda,K. (2002). New polylactide/ layered silicate nanocomposite. Preparation characterization and properties. *Macromolecule*

Ray,S.S., Okamoto, M. (2003). Polymer/layered silicate nanocomposites: a review from preparation to processing. *Prog. Polym. Sci*. 28. pp. 1539–1641.

Rausell,C.J.A., Serratosa,J.M. (1987). Reactions of clays with organic substances. In: Newman ACD, editor. Chemistry of clays and clay minerals, pp. 371.

Salahuddin,N., Shehata,M. (2001). Poly (methyl methacrylate)-montmorillonite composites: preparation, characterization and properties. vol,42, pp. 8379-8500

Sepe,M.P. (1997). Thermal analysis of polymer, vol 8, pp. 11

Silva,C.D., Canto,L., Visconti,L. (2009). Effect of Extrusion Processing Variables on the Polyethylene/Clay Nanocomposites Rheological Properties, "Chemistry & *Chemical Technology*, Bd. 4, Nr. 1, pp. 61-67

Simoes,P.N., Jorge, F.J.C,. Pedro, M.F.O.G., Gil,M.H. (2009). Comparative non-isothermal kinetic analysis of thermal degradation of poly(vinyl chloride) prepared by living and conventional free radical polymerization methods," *European Polymer Journal*, Bd. 45, Nr. 7, pp. 1949-1959

Shah,X. and Paul,D.R. (2004). Nylon 6 nanocomposites prepared by a melt mixing masterbatch process. Polymer 45, pp. 2991-3000

Utrucki,L. (2004). Clay-Containing Polymeric Nanocomposite, Rapra Technology Limited

Vaia,R.A. (1996). Microstructural Evaluation of Melt-intercalated Polymer-Organically Modified Layered Silicate Nanocomposites, "*Chemical Material*, Bd. 8, pp. 2628-2635

Vaia,R.A and Giannelis,EP. (2001). Liquid crystal polymer nanocomposites: direct intercalation of thermotropic liquid crystalline polymers into layered silicates. Polymer

Vanderhart,D.L., Asano,A., Gilman,J.W. (2001). NMR measurements related to clay-dispersion quality and organic-modifier stability in nylon-6/clay nanocomposites, *Chemical Material*, Bd. 13, Nr. 10, pp. 3796–3809

Varlot,K., Reynaud,E., Kloppfer,M.H., Vigier,G., Varlet,J. (2001). Journal Polymer Science part B. *Polymer physic*, pp. 1360-1370

Wang,S., Li,Q., Qi,Z. (1998). Studies on silicone rubberrmontmorillonite hybrid composites.Key Eng. Mater. 137, pp. 87–93.

Xi,Y., Frost,R.L., He,H., Kloprogge,T., Bostrom,T. (2005). Modification of Wyoming montmorillonite surfaces using a cationic surfactant.Langmuir, 21, pp. 8675–8680

Xu,X., Wu,Y., Dong,C., Wu,G.Y., Wang,H. (2006). Study on cationic polymerization of isobutylene using electrochemical method, "*European Polymer Journal*, Bd. 42, Nr. 10, pp. 2791-2800

Yano,K., Usuki,A., Okada,A. (1997). Synthesis and Properties of Polyimide-Clay Hybrid Films.*Journal of Applied Polymer Science: Part A, Polym Chem*, 35, pp. 2289-2294

Yusoh,K., Jin,J., Song,M. (2010). Subsurface mechanical properties of polyurethane/organoclay nanocomposite thin films studied by nanoincentation.

Zaikov,G.E., Lomakin,S.M., Dubnikova,I.L., Berezina,S.M. (2005). Kinetic study of polypropylene nanocomposite thermo-oxidative degradation, *Polym. International*, vol.54, pp. 999-1006

Zeng,Q.H., Yu,A.B., Lu,G.Q.M., Paul,D.R. (2005). Clay based polymer nanocomposites: Research and commercial development. *Journal of nanoscience and nanotechnology*, vol.5, pp. 1574-1592

Zhang, L. (2009). Nanotechnology and nanomaterials: Promises for improved tissue regeneration, "*Nanotoday,* Bd. 4, Nr. 1, pp. 66-80

Zuidam,N.J. and Nedovic,V.A. (2010). Encapsulation Technologies for Active Food Ingredients and Food Processing

APPENDIX A Thermogravimetric Analysis

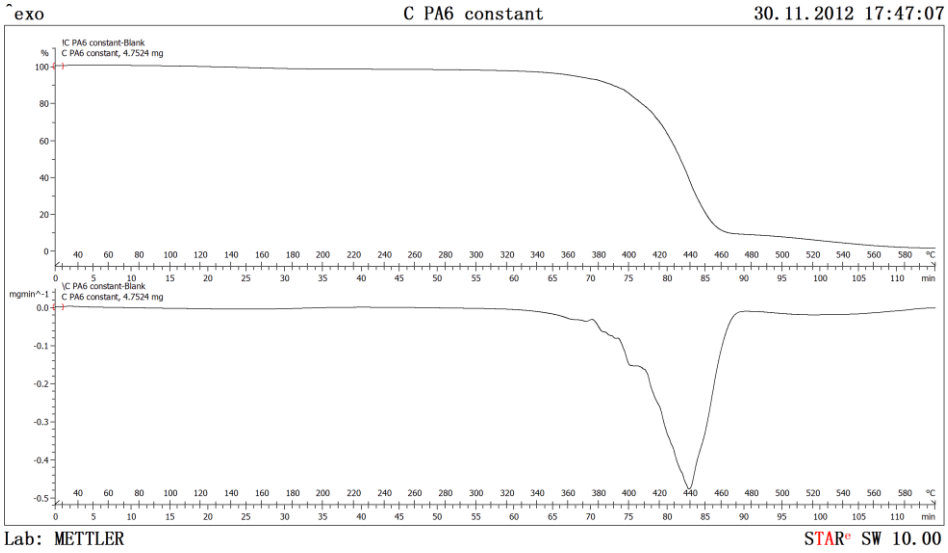

Figure A.1 Conventional (Pure PA6), with $T_{constant}$ at speed 200rpm

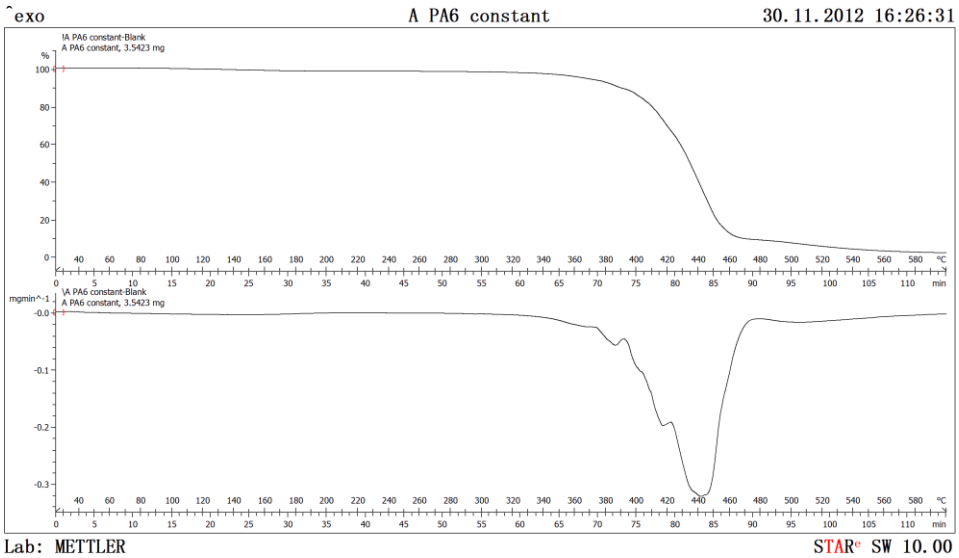

Figure A.2 Auto thermal (Pure PA6), with $T_{constant}$ at speed 200rpm

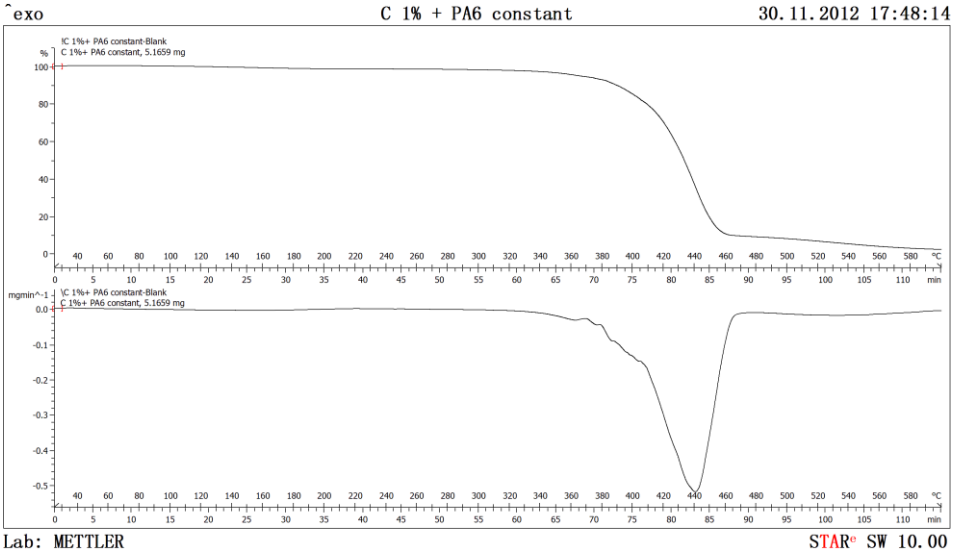

Figure A.3 Conventional (1wt% C20A + PA6), with $T_{constant}$ at speed 200rpm

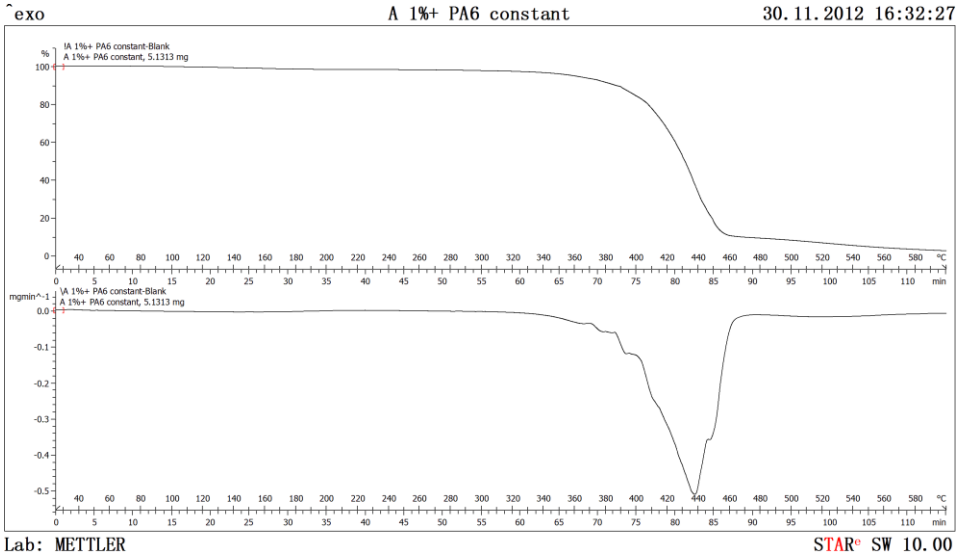

Figure A.4 Auto thermal (1wt% C20A + PA6), with $T_{constant}$ at speed 200rpm

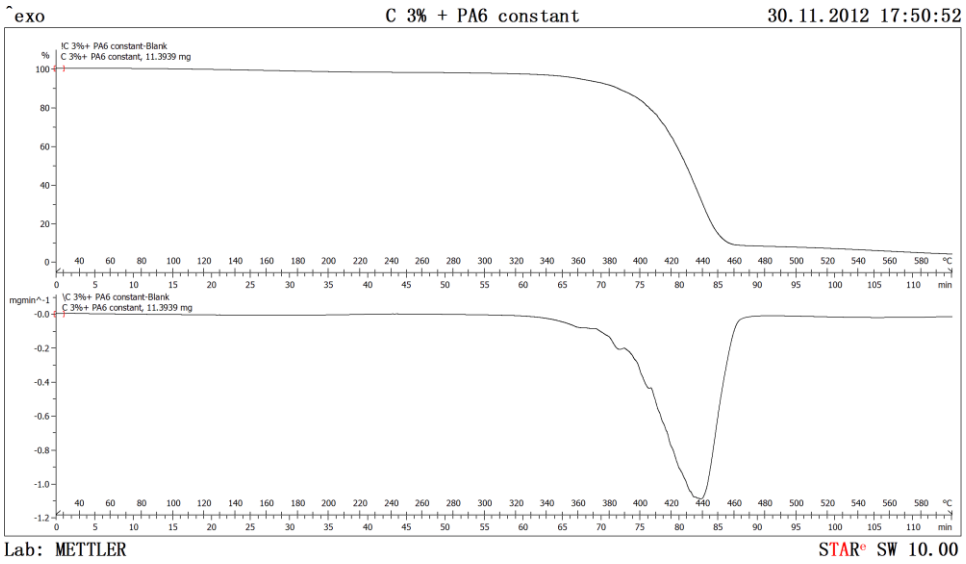

Figure A.5 Conventional (3wt% C20A + PA6), with $T_{constant}$ at speed 200rpm

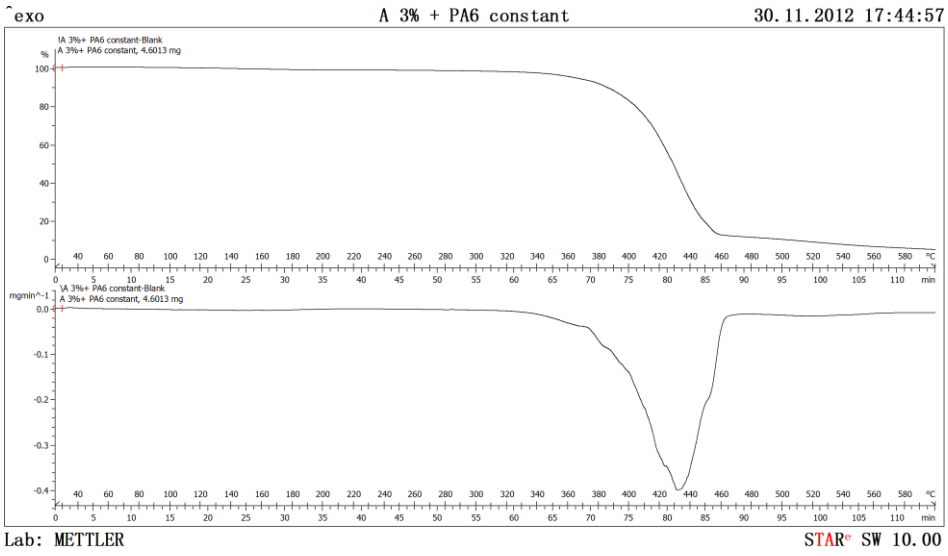

Figure A.6 Auto thermal (3wt% C20A + PA6), with $T_{constant}$ at speed 200rpm

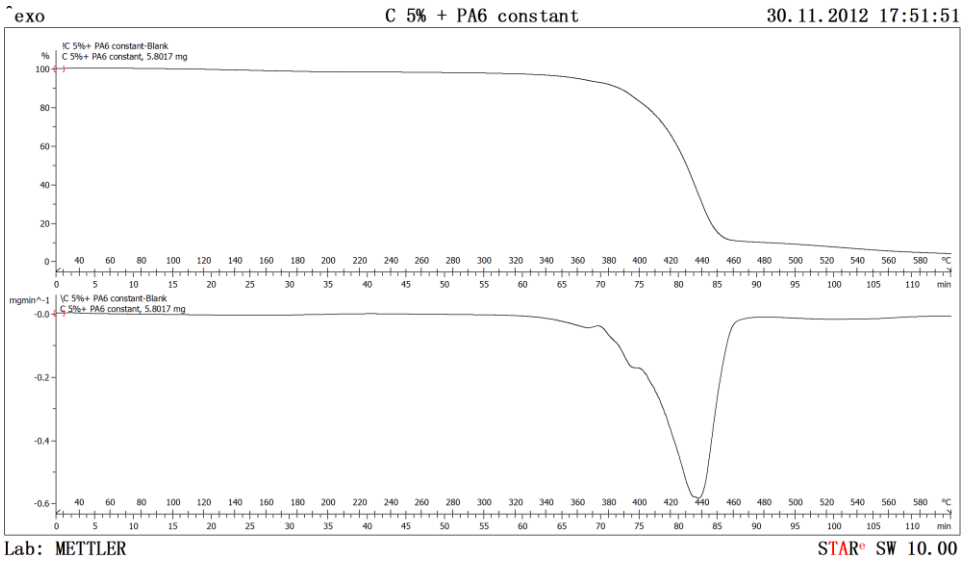

Figure A.7 Conventional (5wt% C20A + PA6), with $T_{constant}$ at speed 200rpm

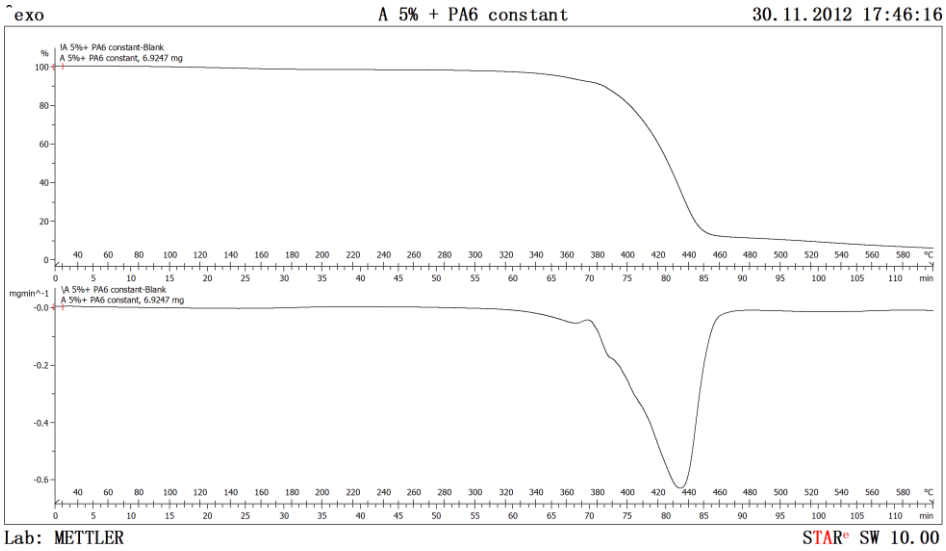

Figure A.8 Auto thermal (5wt% C20A + PA6), with $T_{constant}$ at speed 200rpm

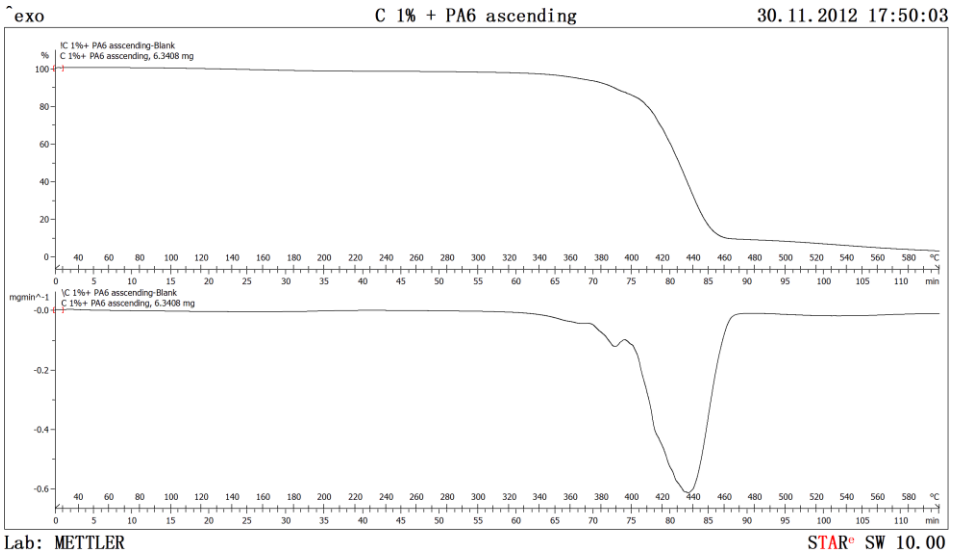

Figure A.9 Conventional (1wt% C20A + PA6), with $T_{ascending}$ at speed 200rpm

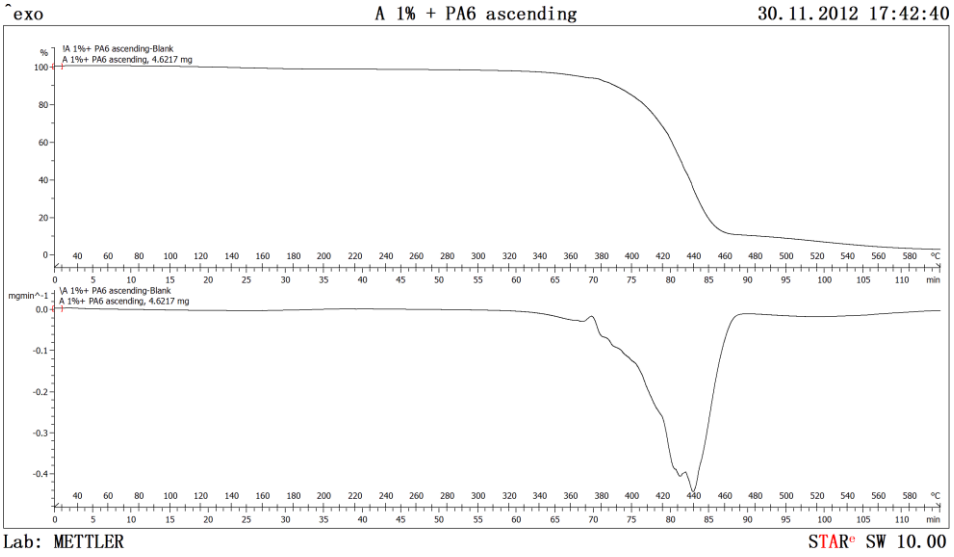

Figure A.10 Auto thermal (1wt% C20A + PA6), with $T_{ascending}$ at speed 200rpm

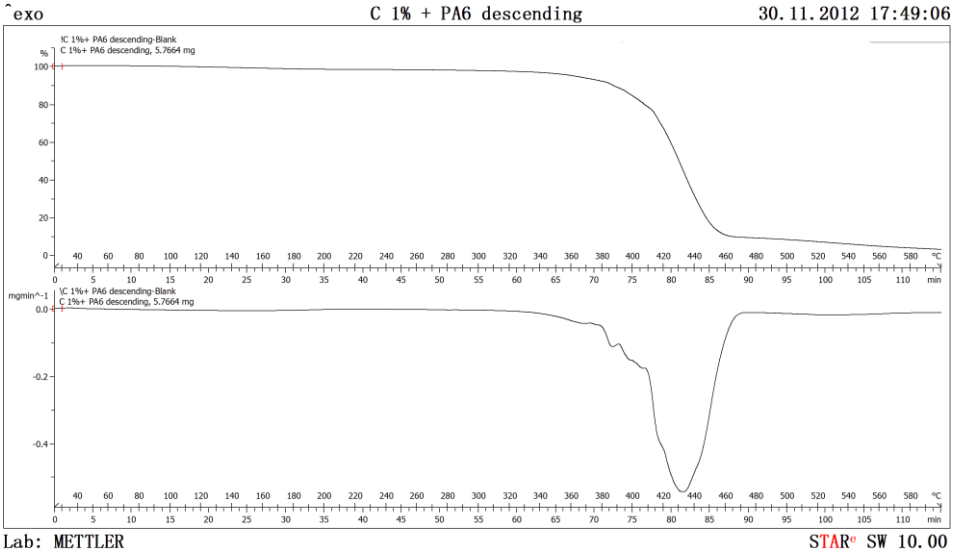

Figure A.11 Conventional (1wt% C20A + PA6), with $T_{descending}$ at speed 200rpm

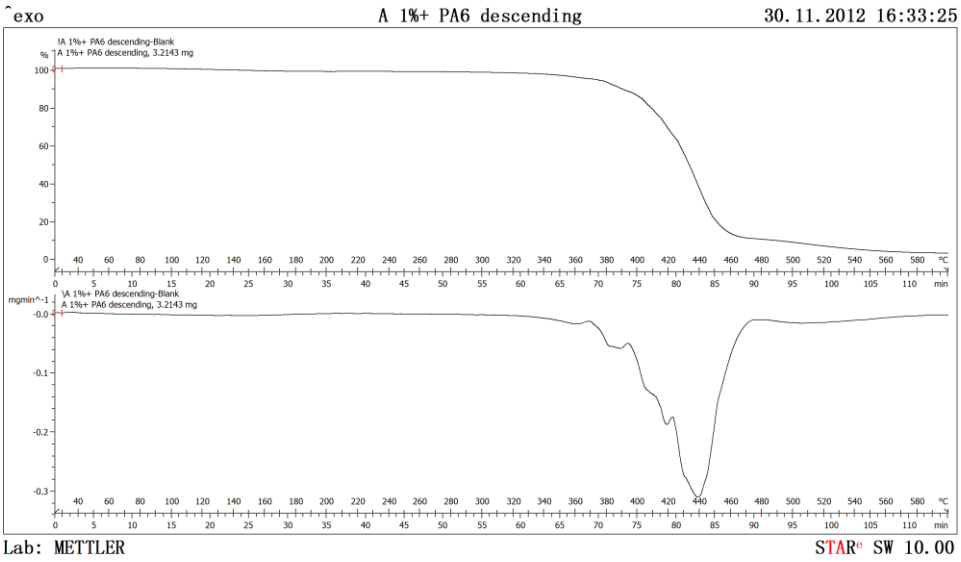

Figure A.12 Auto thermal (1wt% C20A + PA6), with $T_{descending}$ at speed 200rpm

APPENDIX B X-Ray Diffraction Results

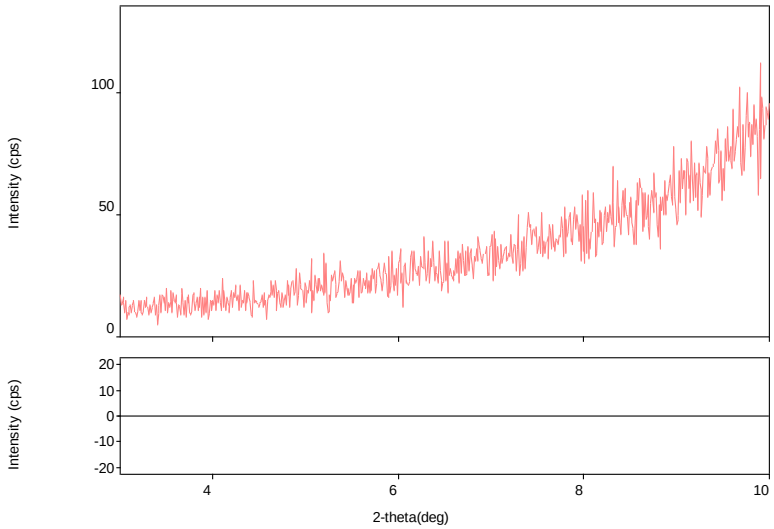

Figure B.1 Conventional (Pure PA6), with $T_{constant}$ at speed 200rpm

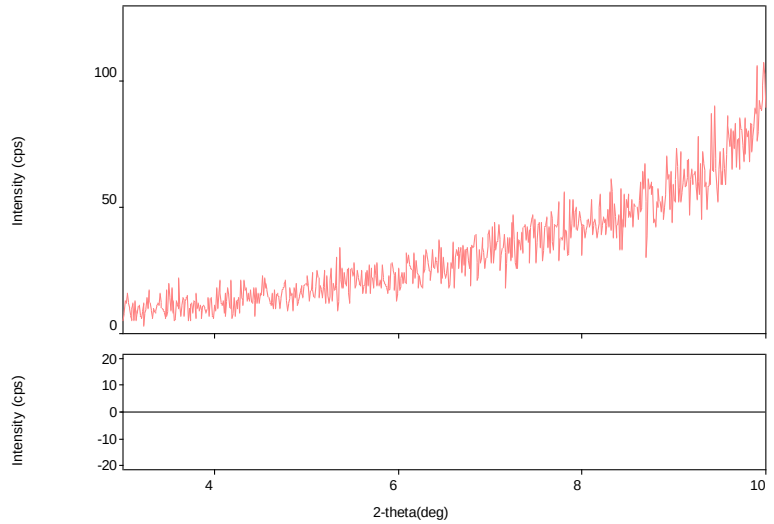

Figure B.2 Auto thermal (Pure PA6), with $T_{constant}$ at speed 200rpm

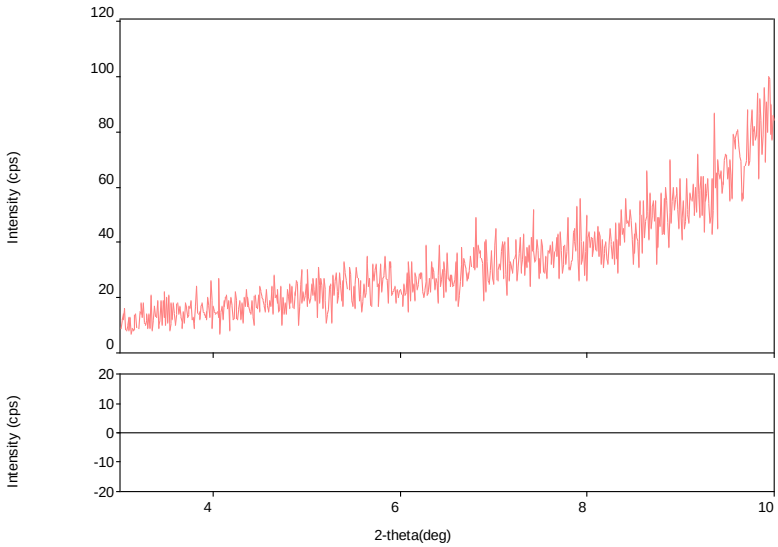

Figure B.3 Conventional (1wt% C20A + PA6), with $T_{constant}$ at speed 200rpm

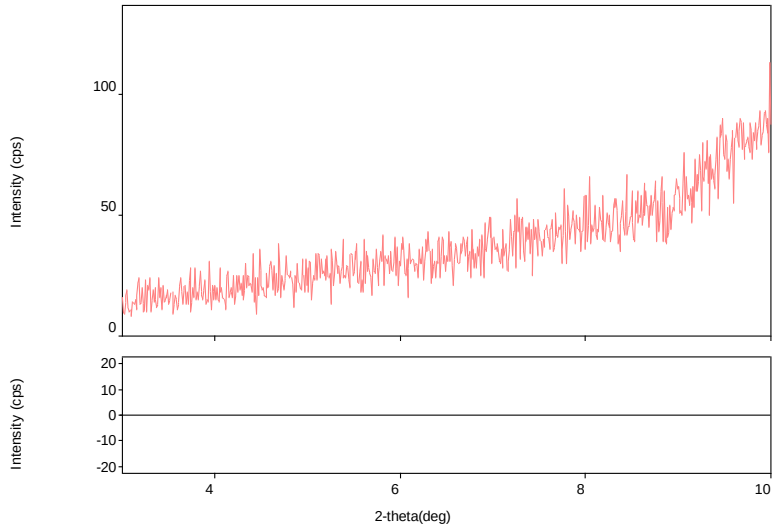

Figure B.4 Auto thermal (1wt% C20A + PA6), with $T_{constant}$ at speed 200rpm

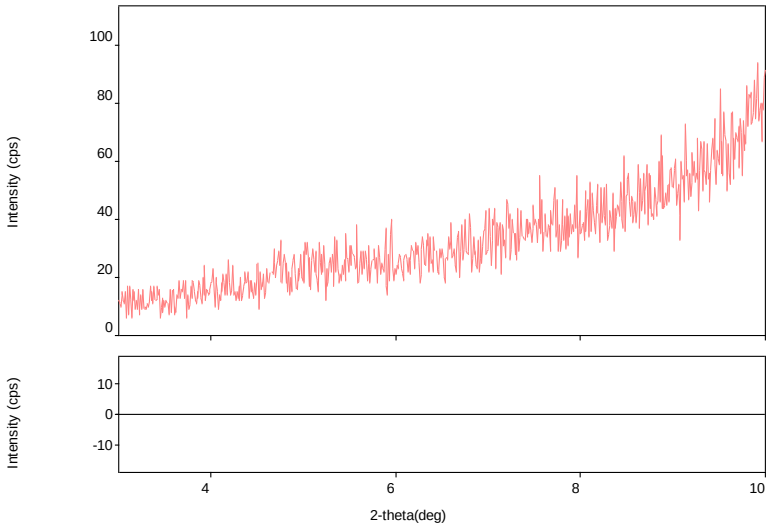

Figure B.5 Conventional (3wt% C20A + PA6), with $T_{constant}$ at speed 200rpm

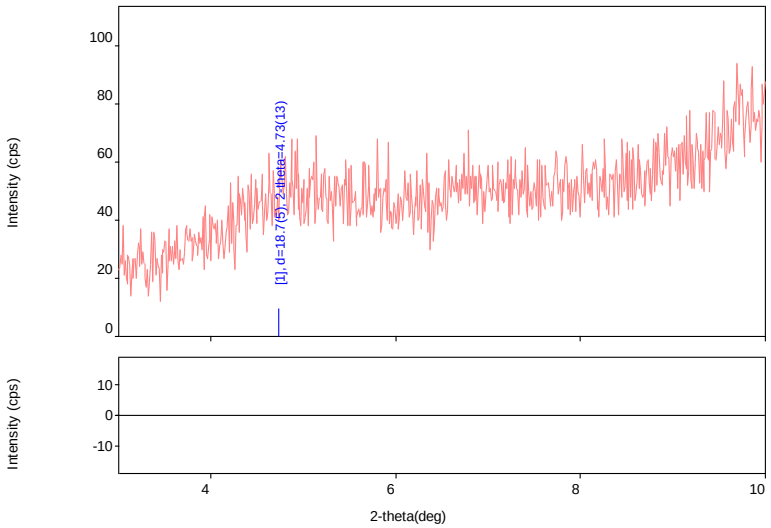

Figure B.6 Auto thermal (3wt% C20A + PA6), with $T_{constant}$ at speed 200rpm

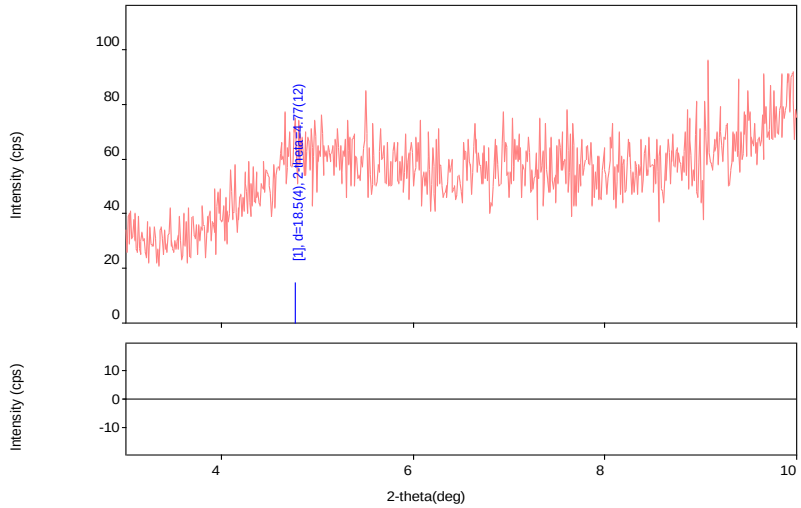

Figure B.7 Conventional (5wt% C20A + PA6), with $T_{constant}$ at speed 200rpm

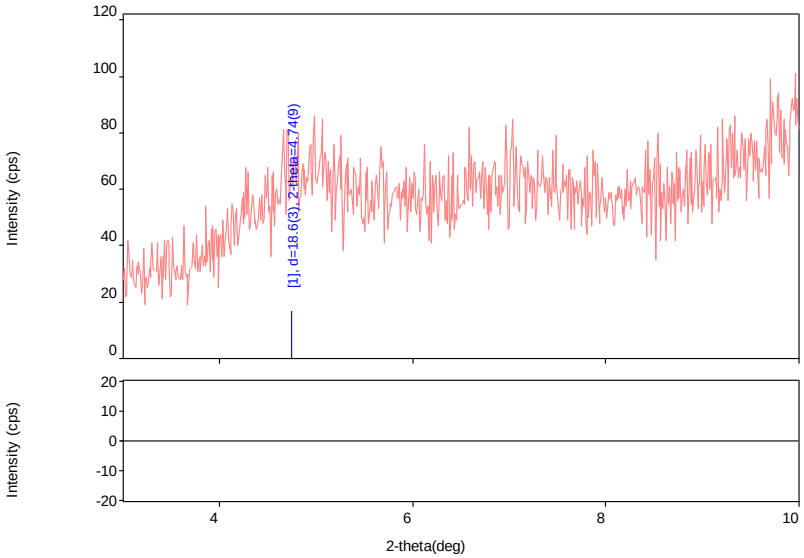

Figure B.8 Auto thermal (5wt% C20A + PA6), with $T_{constant}$ at speed 200rpm

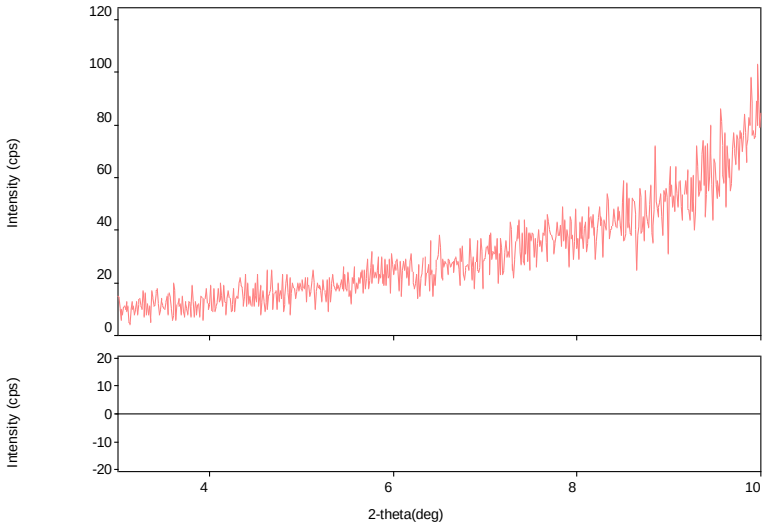

Figure B.9 Conventional (1wt% C20A + PA6), with $T_{ascending}$ at speed 200rpm

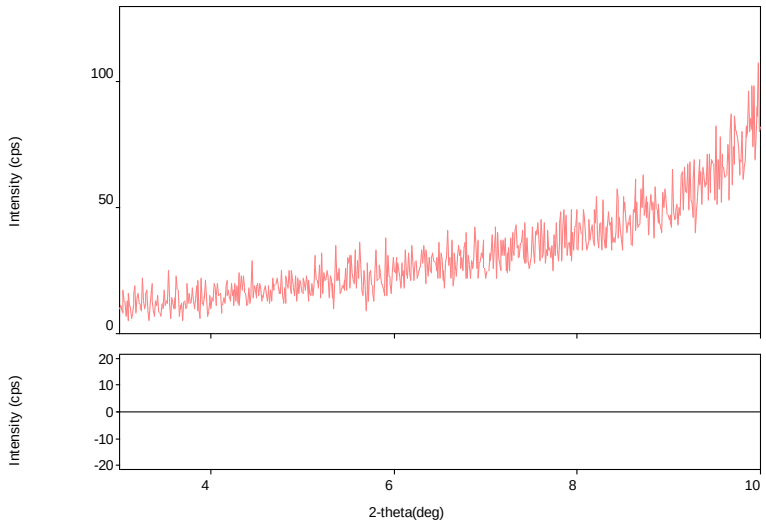

Figure B.10 Auto thermal (1wt% C20A + PA6), with $T_{ascending}$ at speed 200rpm

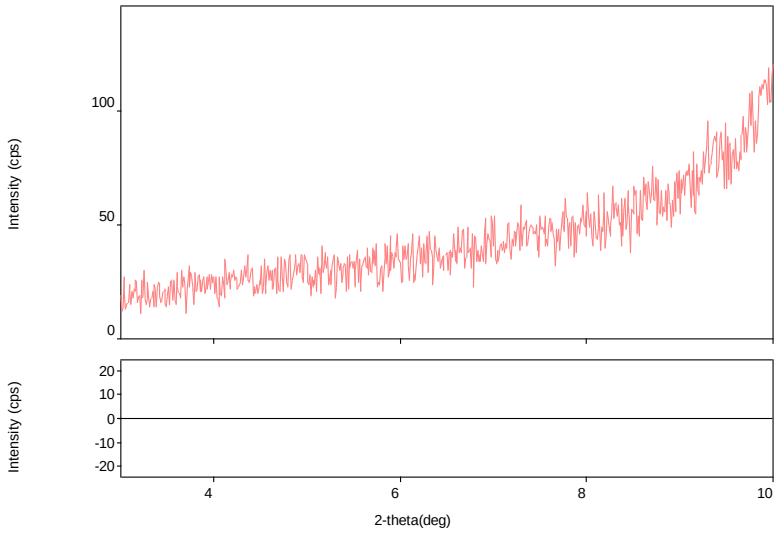

Figure B.11 Conventional (1wt% C20A + PA6), with $T_{descending}$ at speed 200rpm

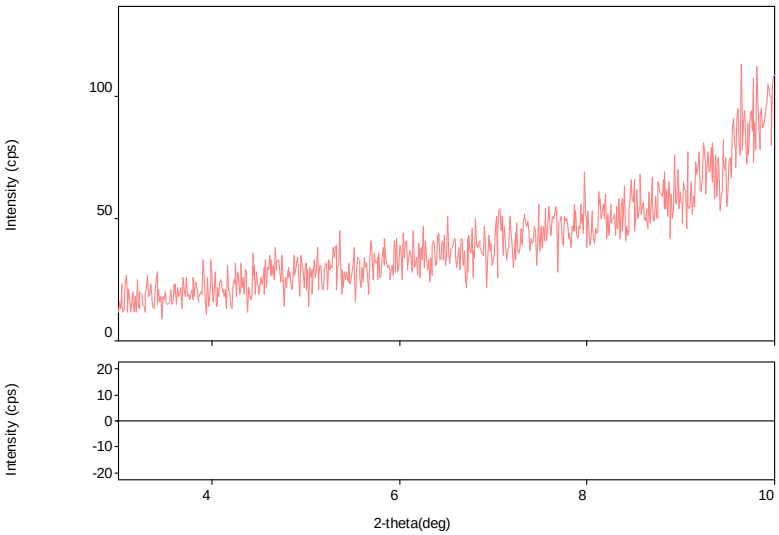

Figure B 12: Auto thermal (1wt% C20A + PA6), with $T_{descending}$ at speed 200rpm